

Positronium Hydride and Tetron

by

Bo Leng

A thesis submitted in partial fulfillment of the requirements for the degree of

Master of Science

Department of Physics

University of Alberta

©Bo Leng, 2020

Abstract

Variational calculations of the ground state of positronium hydride are performed where the various expectation values including the inter-particle distances and the non-relativistic ground state energy. These calculations have been performed using wave function in Gaussian basis with the basis set of 1000. A good agreement with the corresponding values reported in the literature is found for different parameters. Later, we consider the interactions in a mesonic system, referred here to as ‘tetron’, consisting of two heavy quarks and two lighter antiquarks (which may still be heavy in the scale of QCD), i.e. generally $Q_a Q_b \bar{q}_c \bar{q}_d$, and study the existence of bound states below the threshold for decay into heavy meson pairs. At a small ratio of the lighter to heavier quark masses an expansion parameter arises for treatment of the binding in such systems. We find that in the limit where all the quarks and antiquarks are so heavy that a Coulomb-like approximation can be applied to the gluon exchange between all of them, such bound states arise when this parameter is below a certain critical value. We find the parametric dependence of the critical mass ratio on the number of colors N_c , and confirm this dependence by numerical calculations. In particular there are no stable tetrons when all constituents have the same mass. We discuss an application of a similar expansion in the large N_c limit to realistic systems where the antiquarks are light and their interactions are nonperturbative. In this case our findings are in agreement with the recent claims from a phenomenological analysis that a stable $bb\bar{u}\bar{d}$ tetron is likely to exist, unlike those where one or both bottom quarks are replaced by the charmed quark.

Preface

The idea to perform the variational calculation of the PsH using Gaussian wave function is inspired from the following studies:

- M. Puchalski and A. Czarnecki, Phys. Rev. Lett. **101** (2008) 183001.
- M. Puchalski, A. Czarnecki and S. G. Karshenboim, Phys. Rev. Lett. **99** (2007) 203401.

The calculations presented in Chapter 2 are done separately by M. Jamil Aslam, Wen Chen and myself. Chapter 3 is based on the published work Phys. Lett. **B778**, 233 (2018) that is done in collaboration with A. Czarnecki and M. B. Voloshin [1].

Contents

1	Introduction	1
2	Variational Calculation of Binding Energy of PsH	3
2.1	The Variational Ritz Method	3
2.1.1	The Variational Principle	4
2.1.2	The Ritz method	5
2.1.3	Explicitly Correlated Gaussian (ECG) basis	6
2.1.4	The Ritz method for a two state system	8
2.2	Positronium Hydride	11
2.2.1	Introduction	11
2.2.2	PsH Wave function	13
2.2.3	Hamiltonian	15
2.3	Matrix Elements of Hamiltonian for PsH	17
2.3.1	Overlap Integrals	21
2.3.2	Matrix Elements for Coulomb Potential	22
2.3.2.1	Kinetic energy	23
2.3.2.2	Inverse Square of Inter-particle distances	30
2.3.2.3	Inter Particle Distances	30
2.3.3	Numerical Evaluation	31
3	Stability of Tetrons	33
3.4A	solvable model with superheavy quarks	35
3.5	Tetron with superheavy quarks and massless antiquarks	41

4 Conclusion	44
References	46
Appendix: Variational Method coded in Fortran	52
Defining the physical system	54
Solving the system	54
Optimization	57

List of Tables

1	Comparison of our binding energy result with calculations in the literature.	14
2	Expectation values of parameters of PsH and their comparison with [2]. In our work, we compared the values by taking both the 100 and 1000 basis.	32

List of Figures

1	One-gluon exchanges in a tetron.	36
2	Extra binding energy of a tetron (in units of the total binding of two independent $Q\bar{q}$ mesons) as a function of the antiquark/quark mass ratio f . The state with the symmetry w_{++} (circles) is bound strongly than w_{--} (triangles). Even the state w_{++} is no longer bound when the mass ratio exceeds about $f_c \approx 0.152$. The number of colors is $N_c = 3$. . .	41
3	Mass threshold f_c for tetrons as a function of the number of colors. The curve is the fit of the numerically computed values of f_c to the formula in eq. (118).	42
4	Directories and files contained in VM. The boxes with dash line represent a folder and every rigid box is a Fortran file. The blue arrows point to the files which are called by the given file. The blue boxes are used to order the process of the main program. <code>Mystd/prmt.f</code> contains global variables and constants used throughout the program, thus a red arrow is used. The 5 files in the <code>mystd</code> directory are taken from ref. [3].	53
5	Powell Method Optimization Scheme (PMOS).	58

List of Notations and Abbreviations

VM - Variational Method; it is used later as the name of our Fortran program

Ps₂ - Positronium Molecule;

PsH - Positronium Hydride;

GS - Ground State

H₂ - Hydrogen Molecule;

p - Proton;

\hat{H} - Hamiltonian;

\hat{T} - Kinetic Energy;

V - Potential Energy;

CoM - Centre of Mass;

δ - Dirac Delta

a.u. - Atomic Units

Chapter 1

Introduction

Hydrogen atom energy levels and wave functions depend on the reduced mass of the system. The stability of a two-body system is independent of its constituents' mass ratio. This led Stepan Mohorovičić in 1934 to theorize the existence of positronium [4], a system where the proton is replaced by the positron; in 1951 it was discovered by Martin Deutsch [5]. Even before the discovery of positronium, the idea of replacing positron with protons in more complex atoms and molecules was investigated. In almost all such cases it is very difficult or even impossible to analytically solve the Schrödinger equation for these energy levels. In order to check if they form a stable system, Ritz variational principle is used that often yields a set of upper bounds that closely estimate one or more of these energy levels. This dissertation is a step towards the study of the variational calculation of the binding energy of positronium hydride (PsH) and the stability of a tetron (a system consisting of two quarks and two antiquarks, somewhat similar to a positronium molecule).

In Chapter 2 of the dissertation, after giving some details of the variational principle, we use this method in Gaussian basis and combine it with the algorithms for decomposing the Hamiltonian matrix elements and for optimizing the wave function for PsH. Using these optimized wave functions, we calculate the various properties, such as inter-particle distances and the non-relativistic ground state energy and compare them with the ones calculated in [2].

Multi-quark hadrons, whose internal structure apparently goes beyond the standard template of three-quark baryons and quark-antiquark mesons, have recently been observed in various experiments (for a recent review see e.g. [6, 7]). All such exotic hadrons found so far contain a heavy b or c quark and a corresponding antiquark. For this reason they all are unstable with respect to annihilation of a heavy quark-antiquarks pair, even though their rate of dissociation into conventional hadrons can be small. There is a whole spectrum of theoretical models for description of such resonances. In particular the most discussed models for the mesonic ones are the molecular [7, 8], the tetraquark (a recent review can be found in Ref. [9]) and the 'hadro-quarkonium' [10]. A different kind of phenomenology of multi-quark hadrons would be accessible if there existed systems made of two heavy quarks (as opposed to a quark-antiquark pair) and two lighter antiquarks: $Q_a Q_b \bar{q}_c \bar{q}_d$, that would be bound below the threshold for dissociation

into a pair of $Q\bar{q}$ mesons. Such hadrons have been discussed within the quark model for quite some time [11, 12], and the lightest of them can decay only through the weak interaction. In view of special properties of such systems we call them here “tetrons” implying that they in fact are stable (with respect to auto-dissociation) mesons made of four constituents. Their stability is discussed in Chapter 3 of this dissertation. Finally, the main results are summarized in Chapter 4.

The main text is followed by an Appendix presenting the structure of the numerical program used to solve the non-relativistic Schrödinger equation for few-body systems.

Chapter 2

Variational Calculation of Binding Energy of PsH

2.1 The Variational Ritz Method

The Schrödinger equation describes the dynamics of a non-relativistic quantum system. There is no analytical solution for a Coulomb system containing more than two particles. The positronium hydride and the tetron are both four-body systems; therefore we apply the variational method (VM) to obtain an approximate ground state solution of the time-independent Schrödinger equation. This numerical solution can reach high accuracy by optimizing the wave function. The variational method is guaranteed to return an upper bound on the energy.

The ansatz used in our variational method is expressed as a linear combination of basis functions. We employ explicitly correlated Gaussian (ECG) basis function of the type

$$G_m(\vec{r}) \sim \exp \left[-\frac{1}{2} \sum_{j>i=1}^N \alpha_{ij}^m (\vec{r}_i - \vec{r}_j)^2 \right]. \quad (1)$$

The variables α in this type of functions depend on inter-particle distances $|r_i - r_j|$. The correlation factors are adjustable parameters that require optimization such that the energy is optimized.

The Ritz method, discovered by Walther Ritz, applies the variational principle to convert the Schrödinger equation into a generalized eigenvalue problem. This method finds the energy spectrum and the amplitude of each basis function for a given Hamiltonian. This approach is similar to the Galerkin's method of least residual [13]. In general, they belong to a class of mathematical methods for converting a partial differential equation into a matrix problem. Many ideas and techniques from linear algebra can be then applied to solve the original equation numerically.

The amplitude of the basis function is not a variational parameter. The Ritz method computes the amplitude for a chosen set of basis functions. The energy spectrum of the Hamiltonian depends on the variational parameters of each basis function. Finding the lowest energy configuration is a difficult optimization problem. We usually use 200 basis functions, each with six variational parameters so that the dimension of the search space is large. Many optimization algorithms involve the derivatives and the

curvature of the function. It is hard to compute the analytical form of the derivative function of the eigenvalue in terms of the parameters in the ansatz. We choose the Powell method for a multi-dimension optimization task as this algorithm does not require a derivative.

Our algorithm for the variational Ritz method includes the following steps,

1. Prepare the trial wave function;
2. Prepare the Hamiltonian and overlap matrix for the generalized eigenvalue problem;
3. Solve the eigenvalue problem;
4. Use the Powell method to optimize the energy;
5. Repeat step 4 until the desired convergence is reached.

We coded the algorithm above into our VM program. It is based on the Fortran program of Ref. [14] for studying properties of positronium ion (Ps^-) and positronium molecule (Ps_2).

2.1.1 The Variational Principle

The variational method provides an upper bound estimation for each energy level [15]. The variational theorem states that for any normalized state $|\psi\rangle$ (not only an eigenstate of H), the expectation value $\langle\psi|H|\psi\rangle$ is an upper bound to the exact ground state energy, $E_{gs} \leq \langle\psi|H|\psi\rangle$.

We begin the proof by expanding $|\psi\rangle$ on the basis of exact (unknown) eigenstates $|\psi_n\rangle$ of the Hamiltonian

$$|\psi\rangle = \sum_n c_n |\psi_n\rangle, \quad H |\psi_n\rangle = E_n |\psi_n\rangle. \quad (2)$$

Since $|\psi\rangle$ is normalized, we have

$$1 = \langle\psi|\psi\rangle = \left(\sum_m c_m |\psi_m\rangle\right)^\dagger \sum_n c_n |\psi_n\rangle, \quad (3)$$

$$= \sum_{mn} c_m^* c_n \langle\psi_m|\psi_n\rangle = \sum_n |c_n|^2. \quad (4)$$

The expectation value of H in $|\psi\rangle$ is

$$\langle\psi|H|\psi\rangle = \sum_{mn} c_m^* c_n E_n \langle\psi_m|\psi_n\rangle = \sum_n |c_n|^2 E_n. \quad (5)$$

The ground state (GS) energy (E_{gs}) is the smallest eigenvalue

$$E_{gs} \leq E_n, \forall n, \quad (6)$$

thus

$$\langle \psi | H | \psi \rangle \geq \sum_n |c_n|^2 E_{gs} = E_{gs}. \quad (7)$$

By picking a state $|\psi(\alpha_1, \dots, \alpha_n)\rangle$ depending on sufficiently many adjustable parameters, $\alpha_1, \dots, \alpha_n$, we can accurately estimate the ground state energy by minimizing the variational energy $E(\alpha_1, \dots, \alpha_n)$

$$E(\alpha_1, \dots, \alpha_n) \equiv \langle \psi(\alpha_1, \dots, \alpha_n) | H | \psi(\alpha_1, \dots, \alpha_n) \rangle, \quad (8)$$

with respect to these parameters. The condition for finding the minimum ground state energy is the vanishing of the gradient,

$$\frac{\partial E}{\partial \alpha_i}(\alpha_1, \dots, \alpha_n) = 0, \quad (i = 1, \dots, n). \quad (9)$$

The state $|\psi(\alpha_1, \dots, \alpha_n)\rangle$ is often called a “trial wave function” or a “trial state”.

2.1.2 The Ritz method

We apply Ritz method to convert the Schrödinger equation into a generalized eigenvalue problem. This eigenvalue problem might be considered as the matrix form of the Schrödinger equation. We write the trial wave function as

$$|\psi(\alpha_1, \dots, \alpha_n)\rangle = \sum_{m=1}^N W_m G_m. \quad (10)$$

where G_m are the basis functions, N is the basis size, and W_m represents the weight assigned to each basis function. The expectation value of the Hamiltonian is

$$\langle H \rangle = \frac{\int \psi^* H \psi dx}{\int \psi^* \psi dx} = \frac{\sum_{k,m=1}^N W_k^* \langle G_k | H | G_m \rangle W_m}{\sum_{k,m=1}^N W_k^* \langle G_k | G_m \rangle W_m}. \quad (11)$$

Applying the variational condition given in Eq. (9) to the expectation value of the Hamiltonian gives

$$\frac{\partial \langle H \rangle}{\partial W_k} = 0, \quad \frac{\partial \langle H \rangle}{\partial W_k^*} = 0, \quad k = 1, \dots, N. \quad (12)$$

We define elements of Hamiltonian matrix H ,

$$H_{ij} = \langle G_i | H | G_j \rangle, \quad (13)$$

and elements of the overlap matrix S ,

$$S_{ij} = \langle G_i | G_j \rangle. \quad (14)$$

Applying the conditions (12) lead to the same N linear equations

$$\frac{\sum_{m=1} H_{km} W_m \cdot \sum_{k,m=1} W_k^* H_{km} W_m - \sum_{k,m=1} W_k^* H_{km} W_m \cdot \sum_{m=1} S_{km} W_m}{(\sum_{k,m=1} W_k^* S_{km} W_m)^2} = 0, \quad (15)$$

$$\sum_{m=1} H_{km} W_m = \frac{\sum_{k,m=1} W_k H_{km} W_m}{\sum_{k,m=1} W_k^* S_{km} W_m} \cdot \sum_{m=1} S_{km} W_m, \quad (16)$$

$$\frac{\sum_{k,m=1} W_k H_{km} W_m}{\sum_{k,m=1} W_k^* S_{km} W_m} = \langle H \rangle \approx E, \quad (17)$$

$$\sum_{m=1} H_{km} W_m = E \cdot \sum_{m=1} S_{km} W_m, \quad (18)$$

i.e., we obtain the generalized eigenvalue problem

$$HW = ES, \quad (19)$$

and solve it to obtain the eigenvalue E and its eigenvector W . The lowest eigenenergy E will be our estimate for the ground state energy with its eigenvector corresponding to the amplitude W of each basis function in the ground-state ansatz in Eq. (10).

2.1.3 Explicitly Correlated Gaussian (ECG) basis

The heart of the variational method is the choice of a trial function. A basis function in an ansatz is either fixed like B-splines, for example, or the basis function can contain variational parameters. We optimize these variables in the trial function so that it converges to the lowest energy configuration. The Ritz method computes the amplitude associated with each basis function, so only the variational parameters

in each basis function are independent.

Basis functions can be either orthogonal or non-orthogonal. If the choice of basis function is orthonormal, so that $S_{ij} = \delta_{ij}$, where δ_{ij} is the Kronecker delta; S is an identity matrix and eq. (19) is then simply the standard eigenvalue problem $HW = EW$. An advantage of an orthonormal basis is that it simplifies solving the eigenvalue problem.

We employ a non-orthogonal explicitly correlated Gaussian (ECG) basis. The ECG for vanishing angular momentum is

$$G_m(\vec{r}) \sim \exp \left[-\frac{1}{2} \sum_{j>i=1}^N \alpha_{ij}^m (\vec{r}_i - \vec{r}_j)^2 \right]. \quad (20)$$

In a system of several particles, ECG depends explicitly on the inter-particle distance $|\vec{r}_i - \vec{r}_j|$, and the correlation factor α_{ij}^m is a variational parameter. In this non-orthogonal basis, the functions differ only by values of parameters. Since their functional form is identical, it is easier to obtain analytical expressions for the needed matrix elements. Having analytical expressions allows us to reach high numerical precision with a reasonable expense of the computer time. Although a single ECG produces a very inaccurate result, we can increase the accuracy of the solution by simply using more basis functions. This can be easily done with present computation technology. ECG provides accurate energies and expectation value of local operators acting on small distance. The drawback of ECG in comparison with Hylleraas functions (see Section 2.2.1) is that the ECG does not satisfy the so-called cusp condition [16].

To solve the generalized eigenvalue problem, we convert eq. (19) to

$$S^{-1}HW = EW. \quad (21)$$

However, this approach is not computationally favorable since the calculation of the inverse of a large matrix is time consuming. In practice, we utilize the inverse iteration via QR decomposition method to solve the generalized eigenvalue problem (19). We also employ QR update to speed up the optimization process. A detailed discussion of how the general eigenvalue problem is solved can be found in the Appendix.

2.1.4 The Ritz method for a two state system

In case of tetrons which are composed of quarks carrying a color charge, we apply the Ritz method to a 2×2 Hamiltonian describing the interplay of color configurations. The most general form of a real 2×2 Hamiltonian matrix of a two state system is

$$H = \begin{bmatrix} \epsilon_1 & \gamma \\ \gamma & \epsilon_2 \end{bmatrix}, \quad (22)$$

where $\epsilon_1, \epsilon_2, \gamma$ are real operators ensuring the Hermitian property of the Hamiltonian. We substitute this 2×2 Hamiltonian into the Schrödinger equation

$$H \begin{bmatrix} \phi \\ \psi \end{bmatrix} = E \begin{bmatrix} \phi \\ \psi \end{bmatrix}. \quad (23)$$

The two states ϕ and ψ are orthogonal such that $\langle \phi | \psi \rangle = 0$. The expectation value of this Hamiltonian is

$$\langle H \rangle = \frac{\langle \phi | \epsilon_1 | \phi \rangle + \langle \phi | \gamma | \psi \rangle + \langle \psi | \epsilon_2 | \psi \rangle + \langle \psi | \gamma | \phi \rangle}{\langle \phi | \phi \rangle + \langle \psi | \psi \rangle}. \quad (24)$$

ϕ and ψ are both expressed as the linear combination of a certain type of basis function

$$\phi = \sum_{i=1}^N W_i G_i, \quad \psi = \sum_{j=1}^M A_j B_j. \quad (25)$$

Here, G and B are the basis function of ϕ and ψ , respectively and N and M are the basis size of ϕ and ψ , respectively.

The Hamiltonian matrix and overlap matrix have the dimension $(N + M)^2$, and the Hamiltonian matrix contains four square block matrices

$$H = \begin{bmatrix} \epsilon^1 & \gamma^u \\ \gamma^d & \epsilon^2 \end{bmatrix}. \quad (26)$$

The matrix elements of the four block matrices $\epsilon^1, \gamma^u, \gamma^d, \epsilon^2$ are defined as,

$$\epsilon_{il}^1 = \langle G_i | \epsilon_1 | G_l \rangle, \quad \epsilon_{jk}^2 = \langle B_j | \epsilon_2 | B_k \rangle \quad (27)$$

$$\gamma_{ik}^u = \langle G_i | \gamma | B_k \rangle, \quad \gamma_{jl}^d = \langle B_j | \gamma | G_l \rangle. \quad (28)$$

The overlap matrix S contains two block matrices s^1 and s^2 and two zero matrixes,

$$S = \begin{bmatrix} s^1 & 0 \\ 0 & s^2 \end{bmatrix}, \quad (29)$$

where the matrix elements of s^1 and s^2 are given by,

$$s_{il}^1 = \langle G_i^* | G_l \rangle \quad s_{jk}^2 = \langle B_j^* | B_k \rangle. \quad (30)$$

Substitute the equation above into eq. (24) and use the index i for ϕ , l for ϕ^* , j for ψ^* , k for ψ ,

$$\langle H \rangle = \frac{\sum_{i,l=1} W_i^* \epsilon_{il}^1 W_l + \sum_{i,k=1} W_i^* \gamma_{ik}^u A_k + \sum_{j,k=1} A_j^* \epsilon_{jk}^2 A_k + \sum_{j,l=1} A_j^* \gamma_{jl}^d W_l}{\sum_{i,l=1} W_i^* s_{il}^1 W_l + \sum_{j,k=1} A_j^* s_{jk}^2 A_k}. \quad (31)$$

We first apply the variational condition, eq. (9), to the parameters of the ϕ function,

$$\frac{\partial \langle H \rangle}{\partial W_i^*} = 0, \quad i = 1, 2, \dots, N \quad (32)$$

and utilize the identity $\frac{\partial W_i^*}{\partial W_j^*} = \delta_{ij}$. Let $E = \langle H \rangle$, we have N linear equations

$$\sum_l \epsilon_{il}^1 W_l + \sum_k \gamma_{ik}^u A_k = E \sum_l s_{il}^1 W_l. \quad (33)$$

Applying the variational condition

$$\frac{\partial \langle H \rangle}{\partial A_j^*} = 0, \quad j = 1, 2, \dots, M, \quad (34)$$

provides another set of M linear equations,

$$\sum_k \epsilon_{jk}^2 A_k + \sum_l \gamma_{jl}^d W_l = E \sum_k s_{jk}^2 A_k. \quad (35)$$

Combining eq. (33) and eq. (35), we get a generalized eigenvalue problem $Hx = ESx$ with $x = \begin{bmatrix} W \\ A \end{bmatrix}$ being an eigenvector. We apply the same techniques for solving the eigenvalue and eigenvector as in the one-component electrodynamic case.

2.2 Positronium Hydride

2.2.1 Introduction

In 1928, Paul Dirac discovered an equation unifying the theory of special relativity with quantum mechanics [17]. The Dirac equation describes the motion of an electron in the relativistic speed regime. One of the most surprising predictions of this theory is the existence of an anti-particle for every particle. For example, a positron is the antiparticle of an electron. Positron has the same mass as an electron but has an opposite charge. Carl Anderson confirmed the existence of a positron in 1932 by analyzing cosmic rays in a cloud chamber [18].

A natural question to ask is whether there exist neutral entities containing positrons in the universe. John Archibald Wheeler first envisaged a class of short-lived entities composed of positrons and electrons. They are called “Wheeler compounds” and the simplest case is positronium (e^+e^-) [19]. This electron and positron pair has a structure resembling hydrogen with the central proton replaced by a light positron.

Positronium hydride (PsH) is another positronium-containing compound. PsH is a four body system composed of a positron, a proton and two electrons. Aadne Ore was the first to demonstrate the possibility of PsH existence [20] in 1951. He implemented the variational technique developed by Egil Hylleraas [21] for a treatment of Helium. By taking a simple trial wave function with only 4 parameters, Ore obtained a total binding energy 0.75251 hartree, which gives a binding energy of only 0.00251 hartree (relative to separated hydrogen and positronium atoms).

Since then, PsH has become a subject of experimental interest and there exist many studies of its binding energy and other parameters; these efforts are summarized in Table 1. PsH serves as a testing ground for various computation techniques because of its three unique features. First, it is the simplest Coulombic system for examining the ability of a positronium to couple with ordinary matter. Second, the electron-positron correlation plays a significant role in the overall stability of a PsH. Lastly, since PsH is unstable against positronium annihilation, the local behavior of an electron-positron collision must be described.

Standard quantum-chemistry approaches such as the Hartree-Fock method (also called Self consistent field (SCF)) [22, 23, 24] and the configuration interaction (CI) [25, 26, 27, 22, 28] encounter challenges due to the non-negligible electron-positron correlation. While SCF fails to predict a bound state [24], Bromley and Saito both report a slow-convergence problem with the CI method [27, 26]. Strasburger questions the

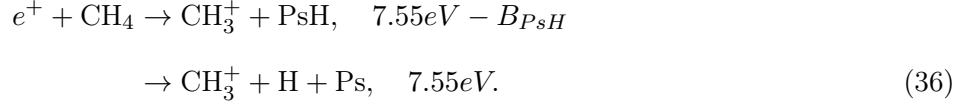
reliability of the CI and SCF implementing on PsH [22]. So far, successful approaches to the PsH ground state problem have been the variational method [2, 20, 29, 30, 31, 32, 33, 34, 35, 36, 37, 38, 39, 40, 41, 42, 43, 44, 45] and the Quantum Monte Carlo method [46, 47, 48, 49, 50]. The core of the variational method is the choice of trial basis function. Rychlewski’s book on the theory and application of explicitly correlated wave functions provides an elaborate description of several types of functions [51]. Among them the Hylleraas [36, 37, 38, 39, 40] and explicitly correlated Gaussians (ECG) [2, 29, 30, 31, 32] basis function are two successful candidates. Although the variational method and Quantum Monte Carlo method have been used to calculate the ground state energy of PsH almost exactly, the trial function contains very many parameters, which provide little insight toward the understanding of properties of PsH. Jiang [48], Bressanini [52], and Le Sech [53] construct a simple compact trial wave function by imposing appropriate physical constraints on the system.

Consensus has not been reached yet regarding the structure of PsH. There are two standard pictures of the configuration of PsH. The first is that it has a diatomic molecular structure similar to H_2 with Ps binding with H [27]. In the second, PsH is considered as a positron bound to a hydrogen negative ion, H^-e^+ . Saito even maintains both atomic H^-e^+ structure and diatomic molecular PsH structure exist [26]. Usukura, Varga, and Suzuki found the electron-positron distance to be slightly larger than in the Ps atom: $3.45a_0$ versus $3a_0$ (a_0 is the Bohr radius), and the average electron-nucleus is $2.31a_0$, which is larger than in the hydrogen atom ($1.5a_0$). Due to this fact, the interpretation of PsH as being simply separated into Ps + H is not supported [32]. Frolov and Smith argue that PsH can be viewed as “the physical sum of the positronium ion (Ps^-) and a hydrogen negative ion (H^-)” [34] since $E_{PsH} \approx E_{Ps^-} + E_{H^-}$.

In continuation of the study of the bound state properties of the PsH, Yan, Ho [54] and Bubin, Varga [55] took the next step of considering relativistic and QED effects to the binding energy of this system. Frolov studied the fine and hyperfine structures of PsH [34].

Experimentally, PsH can be naturally formed and then annihilated in hydrogen star and is applicable to astrophysical models of positron annihilation from galactic center and solar flare [56]. While PsH has been shown to have a bound state with an energy below the lowest dissociation channel (Ps + H), it is not stable against positronium annihilation, which happens within a time on the order of nanoseconds. Laboratory observations of this short lifetime of PsH are not available with the present detection technology. Drachman and Schrader find the binding energy of PsH (B_{PsH}) to be 1.1 ± 0.2 eV [57]. PsH was created in the collision

between positrons and methane



Schrader et al estimates the binding energy of PsH by comparing the impact energy for $e^+ + \text{CH}_4 \rightarrow \text{CH}_3^+ + \text{PsH}$ with $e^+ + \text{CH}_4 \rightarrow \text{CH}_3^+ + \text{Ps} + \text{H}$. The detection of CH_3^+ ion below the threshold for the production of $\text{CH}_3^+ + \text{H} + \text{Ps}$ signals the formation of PsH. Given the large energy spread and uncertainty of the positron beam, the accuracy of their result is limited and also this result deviates from the present theoretical values.

2.2.2 PsH Wave function

PsH contains a heavy nucleus, a positron and two indistinguishable electrons. To construct the trial wave function, it is necessary to consider the symmetry of the system. From the Pauli exclusion principle, the total wave function should be antisymmetrized with respect to the exchange of two electrons. It is shown in [36] that the triplet state of PsH is not stable against dissociation to a hydrogen and a positronium. The total trial wave function Ψ has an antisymmetric spin part and a symmetric spatial wave function ψ ,

$$\Psi = \chi_{\uparrow}^1 \chi_{\uparrow}^2 (\chi_{\downarrow}^3 \chi_{\uparrow}^4 - \chi_{\uparrow}^3 \chi_{\downarrow}^4) \psi, \tag{37}$$

$$\psi = \sum_{i=1}^N c_i (1 + P_{34}) |G_i^{1234}\rangle, \tag{38}$$

where we have absorbed the factor of $\frac{1}{\sqrt{2}}$ into the normalization constant c_i . The indices $\{1, 2\}$ are for $\{p^+, e^+\}$, $\{3, 4\}$ for $\{e^-, e^-\}$ and P_{34} is the permutation operator for the two identical fermions. In terms of relative coordinates, the ground state description in an explicitly correlated Gaussian basis takes the form

$$|G_i^{1234}\rangle \equiv \exp(-a_i r_{12}^2 - b_i r_{13}^2 - c_i r_{14}^2 - d_i r_{23}^2 - e_i r_{24}^2 - f_i r_{34}^2), \tag{39}$$

where i is the index of the basis.

The variational method optimizes the set of parameters $\{a_i, b_i, c_i, d_i, e_i, f_i; i = 1, \dots, N\}$ to obtain an

Table 1: Comparison of our binding energy result with calculations in the literature.

Group/Technique	Terms	Total E (hartree)	Binding (eV)
Current work/Variational ECG	1000	-0.788870345206	1.0577
Ore (1951) [20]/ Variational exponential	2	-0.75251	0.068301
Neamtan (1962)[41] / Variational exponential	2	-0.7584	0.2286
Goldanskii(1965) [24] /SCF	-	-0.6677	-2.2395
Ludwig(1966)[25]/ CI	9	-0.7590	0.2449
Lebeda (1969) [42] /Variational	12	-0.7742	0.6585
Houston (1973) [44] /Variational	56	-0.7747	0.6725
Navin (1974) [43]/ Variational	17	-0.7792	0.7946
Page (1974) [45] / Variational	70	-0.78679	1.0011
Clary(1976)[28]/CI	67	-0.784161	0.929568
Ho (1978) [39]/ Variational Hylleraas	210	-0.787525	1.02112
Ho (1986) [40]/ Variational Hylleraas	396	-0.788945	1.05975
Schrader (1992) [57]/ Experiment	—	-0.790	1.1 ± 0.2
Strasburger (1995) [22]/CI	—	-0.7637	0.3728
Strasburger (1995) [22]/SCF	-	-0.6669	-2.261
Saito (1995) [23]/ Restricted Hartree-Fock	-	0.776	0.70
Yoshida (1996) [50]/ DMC	-	-0.7891	1.06
Frolov (1997) [33]/ Variational James-Coolidge	924	-0.7891369	1.064969
Frolov (1997) [34]/ Variational Kolesnikov-Tarasov	—	-0.7891794	1.066126
Bressanini (1998)[47]/DMC	—	-0.789175	1.06601
Jiang (1998) [48]/DMC	-	-0.78918	1.0661
Jiang (1998)[48]/ Variational Monte Carlo	1	-0.7774	0.7456
Le Sech (1998) [53] / Variational Monte Carlo	1	-0.7723	0.6068
Strasburger (1998)[31] /Variational ECG	332	-0.789185	1.066278
Usukura (1998)[32]/ Variational ECG with SVM	1600	-0.7891965536	1.066592513
Yan (1999) [38]/ Variational Hylleraas	5741	-0.7891967051	1.066596635
Mella (1999) [49]/DMC	—	-0.78915	1.0653
Ryzhikh (1999) [58] / Variational ECG	750	-0.7891960	1.066577
Bromley (2001)[27]/CI	95324	-0.7867761	1.000729
Saito (2003)[26]/MRCI	13230	-0.786793	1.0019
Bressanini (2003) [52]/ Variational Monte Carlo	1	-0.786073	0.981596
Van Reeth (2004) [37]/ Variational Hylleraas	721	-0.789156	1.0655
Chiesa (2004)[46]/ QMC	—	-0.784620	0.942058
Mitroy (2006)[2]/Variational ECG with SVM	1800	-0.789196740	1.06659758
Bubin (2006) [29]/Variational ECG	5000	-0.789196765251	1.066598271959
Frolov (2010) [35]/ Variational semi-exponential	84	-0.788516419	1.04808511
Woods (2015) [36]/ Variational Hylleraas	1505	-0.789189725	1.066406705

upper bound on the eigenenergy. We define a ECG basis in terms of those non-linear parameters

$$G(a, b, c, d, e, f) \equiv \exp(-ar_{12}^2 - br_{13}^2 - cr_{14}^2 - dr_{23}^2 - er_{24}^2 - fr_{34}^2). \quad (40)$$

The permutation operator P_{34} swaps indices $\{3, 4\}$ giving the wave function

$$|G_i^{1243}\rangle \equiv P_{34} |G_i^{1234}\rangle = \exp(-a_i r_{12}^2 - b_i r_{14}^2 - c_i r_{13}^2 - d_i r_{24}^2 - e_i r_{23}^2 - f_i r_{34}^2) \quad (41)$$

$$= \exp(-a_i r_{12}^2 - c_i r_{13}^2 - b_i r_{14}^2 - e_i r_{23}^2 - d_i r_{24}^2 - f_i r_{34}^2) \quad (42)$$

$$= G(a_i, c_i, b_i, e_i, d_i, f_i) \quad (43)$$

and the total wave function is

$$\psi = \sum_{i=1}^N c_i (|G_i^{1234}\rangle + |G_i^{1243}\rangle) \quad (44)$$

with N signifying the number of basis functions.

2.2.3 Hamiltonian

In order to write the Hamiltonian, there are different approaches adopted in the literature. For example in reference [59] the proton, being heavy compared to other constituents, is considered to be at rest and all the other particles are moving with respect to it. However, in our approach, we will follow the analogy of Ps_2 where the motion of all the four bodies is considered. The corresponding Hamiltonian of this system can be written as

$$\begin{aligned} \hat{H} &= \sum_{i=1}^4 \frac{\hat{p}_i^2}{2m_i} + \sum_{i<j} V(r_{ij}) \\ &= \frac{\hat{p}_1^2}{2m_1} + \frac{\hat{p}_2^2}{2m_2} + \frac{\hat{p}_3^2}{2m_3} + \frac{\hat{p}_4^2}{2m_4} + \alpha \sum_{i<j} \left[\frac{z_i z_j}{r_{ij}} \right] \\ &= \frac{\vec{\nabla}_{\vec{A}_1}^2}{2m_1} + \frac{\vec{\nabla}_{\vec{A}_2}^2}{2m_2} + \frac{\vec{\nabla}_{\vec{A}_3}^2}{2m_3} + \frac{\vec{\nabla}_{\vec{A}_4}^2}{2m_4} + \alpha \sum_{i<j} \left[\frac{z_i z_j}{r_{ij}} \right] \end{aligned} \quad (45)$$

where, as in Eq. (38), we use indices $\{1, 2\}$ for the $\{p, e^+\}$ and $\{3, 4\}$ for $\{e^-, e^-\}$. Parameters z_i correspond to the charge index which is -1 for e^- and $+1$ for $\{e^+, p\}$. We know that the masses of electron and positron are equal and we can write $m_2 = m_3 = m_4 = m$. In Eq. (45) $\alpha \simeq 1/137$ denotes

the fine structure constant and the kinetic energy operator is written in terms of the the LAB coordinates \vec{A}_i . The potential energy operator is expressed in the form of inter-particle distances $r_{ij} = \sqrt{(\vec{A}_i - \vec{A}_j)^2}$. As the trial wave function is expressed in terms of the inter-particle distances, it is necessary to write the kinetic energy operator

$$\hat{T} = -\frac{1}{2} \left[\frac{\nabla_{\vec{A}_1}^2}{m_1} + \frac{\nabla_{\vec{A}_2}^2}{m_2} + \frac{\nabla_{\vec{A}_3}^2}{m_3} + \frac{\nabla_{\vec{A}_4}^2}{m_4} \right], \quad (46)$$

in terms of these inter-particle distances instead of the LAB coordinates. To do this, introduce the CoM (center of mass) coordinates,

$$\vec{R} = \frac{1}{M} \left(m_1 \vec{A}_1 + m_2 \vec{A}_2 + m_3 \vec{A}_3 + m_4 \vec{A}_4 \right), \quad (47)$$

where $M = m_1 + m_2 + m_3 + m_4$ is the total mass. The three independent relative coordinates are

$$\begin{aligned} \vec{r}_{12} &= \vec{A}_2 - \vec{A}_1, \\ \vec{r}_{13} &= \vec{A}_3 - \vec{A}_1, \\ \vec{r}_{14} &= \vec{A}_4 - \vec{A}_1. \end{aligned} \quad (48)$$

In terms of these coordinates, one writes

$$\begin{aligned} \vec{\nabla}_{\vec{A}_1} &= \frac{\partial \vec{R}}{\partial \vec{A}_1} \frac{\partial}{\partial \vec{R}} + \frac{\partial \vec{r}_{12}}{\partial \vec{A}_1} \frac{\partial}{\partial \vec{r}_{12}} + \frac{\partial \vec{r}_{13}}{\partial \vec{A}_1} \frac{\partial}{\partial \vec{r}_{13}} + \frac{\partial \vec{r}_{14}}{\partial \vec{A}_1} \frac{\partial}{\partial \vec{r}_{14}} \\ &= \frac{m_1}{M} \vec{\nabla}_{\vec{R}} - \vec{\nabla}_{\vec{r}_{12}} - \vec{\nabla}_{\vec{r}_{13}} - \vec{\nabla}_{\vec{r}_{14}}. \end{aligned} \quad (49)$$

Similarly,

$$\begin{aligned} \vec{\nabla}_{\vec{A}_2} &= \frac{m_2}{M} \vec{\nabla}_{\vec{R}} - \vec{\nabla}_{\vec{r}_{12}}, \\ \vec{\nabla}_{\vec{A}_3} &= \frac{m_3}{M} \vec{\nabla}_{\vec{R}} - \vec{\nabla}_{\vec{r}_{13}}, \\ \vec{\nabla}_{\vec{A}_4} &= \frac{m_4}{M} \vec{\nabla}_{\vec{R}} - \vec{\nabla}_{\vec{r}_{14}}. \end{aligned} \quad (50)$$

As the motion of the CoM does not have any effect on the internal dynamics of the system, the corre-

sponding kinetic energy operator $\vec{\nabla}_{\vec{R}}$ can be ignored. Doing so, we have

$$\begin{aligned}\vec{\nabla}_{\vec{A}_1}^2 &= \vec{\nabla}_{\vec{r}_{12}}^2 + \vec{\nabla}_{\vec{r}_{13}}^2 + \vec{\nabla}_{\vec{r}_{14}}^2 + 2\vec{\nabla}_{\vec{r}_{12}} \cdot \vec{\nabla}_{\vec{r}_{13}} + 2\vec{\nabla}_{\vec{r}_{12}} \cdot \vec{\nabla}_{\vec{r}_{14}} + 2\vec{\nabla}_{\vec{r}_{13}} \cdot \vec{\nabla}_{\vec{r}_{14}}, \\ \vec{\nabla}_{\vec{A}_2}^2 &= \vec{\nabla}_{\vec{r}_{12}}^2, \quad \vec{\nabla}_{\vec{A}_3}^2 = \vec{\nabla}_{\vec{r}_{13}}^2, \quad \vec{\nabla}_{\vec{A}_4}^2 = \vec{\nabla}_{\vec{r}_{14}}^2.\end{aligned}\tag{51}$$

Thus, the kinetic energy operator becomes

$$\begin{aligned}\hat{T} &= -\frac{1}{2} \left[\frac{\vec{\nabla}_{\vec{r}_{12}}^2 + \vec{\nabla}_{\vec{r}_{13}}^2 + \vec{\nabla}_{\vec{r}_{14}}^2 + 2\vec{\nabla}_{\vec{r}_{12}} \cdot \vec{\nabla}_{\vec{r}_{13}} + 2\vec{\nabla}_{\vec{r}_{12}} \cdot \vec{\nabla}_{\vec{r}_{14}} + 2\vec{\nabla}_{\vec{r}_{13}} \cdot \vec{\nabla}_{\vec{r}_{14}}}{m_1} + \frac{\vec{\nabla}_{\vec{r}_{12}}^2}{m_2} + \frac{\vec{\nabla}_{\vec{r}_{13}}^2}{m_3} + \frac{\vec{\nabla}_{\vec{r}_{14}}^2}{m_4} \right], \\ &= -\frac{1}{2} \left[\frac{1}{\mu_{12}} \vec{\nabla}_{\vec{r}_{12}}^2 + \frac{1}{\mu_{13}} \vec{\nabla}_{\vec{r}_{13}}^2 + \frac{1}{\mu_{14}} \vec{\nabla}_{\vec{r}_{14}}^2 + \frac{2}{m_1} \left(\vec{\nabla}_{\vec{r}_{12}} \cdot \vec{\nabla}_{\vec{r}_{13}} + \vec{\nabla}_{\vec{r}_{12}} \cdot \vec{\nabla}_{\vec{r}_{14}} + \vec{\nabla}_{\vec{r}_{13}} \cdot \vec{\nabla}_{\vec{r}_{14}} \right) \right],\end{aligned}\tag{52}$$

where $\mu_{ij} = \frac{m_i m_j}{m_i + m_j}$ is the reduced mass. We adopt such units that $m_1 = m_p \simeq 1836.15$, $m_1 = m_2 = m_3 = m_e = 1$; therefore, reduced masses are $\mu_{12} = \mu_{13} = \mu_{14}$.

Hence, Eq. (52) becomes

$$\hat{T} = -\frac{1}{2\mu_{12}} \left[\vec{\nabla}_{\vec{r}_{12}}^2 + \vec{\nabla}_{\vec{r}_{13}}^2 + \vec{\nabla}_{\vec{r}_{14}}^2 \right] - \frac{1}{m_1} \left[\vec{\nabla}_{\vec{r}_{12}} \cdot \vec{\nabla}_{\vec{r}_{13}} + \vec{\nabla}_{\vec{r}_{12}} \cdot \vec{\nabla}_{\vec{r}_{14}} + \vec{\nabla}_{\vec{r}_{13}} \cdot \vec{\nabla}_{\vec{r}_{14}} \right]\tag{53}$$

The potential energy operator for PsH is

$$\hat{V} = \frac{z_1 z_2}{r_{12}} + \frac{z_3 z_4}{r_{34}} + \frac{z_1 z_3}{r_{13}} + \frac{z_1 z_4}{r_{14}} + \frac{z_2 z_3}{r_{23}} + \frac{z_2 z_4}{r_{24}}\tag{54}$$

where $z_1 = z_2 = 1, z_3 = z_4 = -1$ are the charges of each constituent and the fine structure constant is absorbed in the unit of length. The central potential is simply

$$\hat{V} = \frac{1}{r_{12}} + \frac{1}{r_{34}} - \frac{1}{r_{13}} - \frac{1}{r_{14}} - \frac{1}{r_{23}} - \frac{1}{r_{24}},\tag{55}$$

in our case.

2.3 Matrix Elements of Hamiltonian for PsH

In order to construct the general eigenvalue problem, we need to find the algebraic formula for each matrix

element. The evaluation of matrix element involves the calculation of Gaussian integral. The fundamental form of a Gaussian integral for all matrix elements is

$$I(a, b, c, d, e, f) = \langle \psi_i^{1234} | \psi_j^{1234} \rangle = \int d^3\vec{r}_{12} d^3\vec{r}_{13} d^3\vec{r}_{14} \exp(-ar_{12}^2 - br_{13}^2 - cr_{14}^2 - dr_{23}^2 - er_{24}^2 - fr_{34}^2). \quad (56)$$

In order to evaluate these integrals first shift the coordinates [60]

$$\begin{aligned} \vec{r}_{12} &= \vec{x} + \alpha_1 \vec{y} + \alpha_2 \vec{z}, \\ \vec{r}_{13} &= \vec{y} + \alpha_3 \vec{z}, \\ \vec{r}_{14} &= \vec{z}. \end{aligned} \quad (57)$$

The Jacobian corresponding to these transformations is 1 and the α_1 , α_2 and α_3 are constants to be determined later. Write

$$\begin{aligned} \vec{r}_{23} &= \vec{r}_{13} - \vec{r}_{12} = -\vec{x} + (1 - \alpha_1) \vec{y} + (\alpha_3 - \alpha_2) \vec{z}, \\ \vec{r}_{24} &= \vec{r}_{14} - \vec{r}_{12} = -\vec{x} - \alpha_1 \vec{y} + (1 - \alpha_2) \vec{z}, \\ \vec{r}_{34} &= \vec{r}_{14} - \vec{r}_{13} = -\vec{y} + (1 - \alpha_3) \vec{z}. \end{aligned} \quad (58)$$

In these coordinates,

$$\begin{aligned} -ar_{12}^2 &= -a(\vec{x} + \alpha_1 \vec{y} + \alpha_2 \vec{z})^2 = -a(x^2 + \alpha_1^2 y^2 + \alpha_2^2 z^2 + 2\alpha_1 \vec{x} \cdot \vec{y} + 2\alpha_2 \vec{x} \cdot \vec{z} + 2\alpha_1 \alpha_2 \vec{y} \cdot \vec{z}), \\ -br_{13}^2 &= -b(\vec{y} + \alpha_3 \vec{z})^2 = -b(y^2 + \alpha_3^2 z^2 + 2\alpha_3 \vec{y} \cdot \vec{z}), \\ -cr_{14}^2 &= -c(\vec{z})^2 = -cz^2, \\ -dr_{23}^2 &= -d(-\vec{x} + (1 - \alpha_1) \vec{y} + (\alpha_3 - \alpha_2) \vec{z})^2 = -d[x^2 + (1 - \alpha_1)^2 y^2 + (\alpha_3 - \alpha_2)^2 z^2 - 2(1 - \alpha_1) \vec{x} \cdot \vec{y} \\ &\quad - 2(\alpha_3 - \alpha_2) \vec{x} \cdot \vec{z} + 2(1 - \alpha_1)(\alpha_3 - \alpha_2) \vec{y} \cdot \vec{z}], \\ -er_{24}^2 &= -e(-\vec{x} - \alpha_1 \vec{y} + (1 - \alpha_2) \vec{z})^2 = -e[x^2 + \alpha_1^2 y^2 + (1 - \alpha_2)^2 z^2 + 2\alpha_1 \vec{x} \cdot \vec{y} \\ &\quad - 2(1 - \alpha_2) \vec{x} \cdot \vec{z} - 2\alpha_1(1 - \alpha_2) \vec{y} \cdot \vec{z}], \\ -fr_{34}^2 &= -f(-\vec{y} + (1 - \alpha_3) \vec{z})^2 = -f[y^2 + (1 - \alpha_3)^2 z^2 - 2(1 - \alpha_3) \vec{y} \cdot \vec{z}]. \end{aligned} \quad (59)$$

In line with reference [60], put $\alpha_4 = 1 - \alpha_2$, $\alpha_5 = 1 - \alpha_3$, $\alpha_3 - \alpha_2 = \alpha_4 - \alpha_5$ and collect the coefficients of different dot products in Eq. (59) and later set them equal to zero without loss of generality. This leads to

$$\begin{aligned}
(\vec{x} \cdot \vec{y}) [-2a\alpha_1 + 2d(1 - \alpha_1) - 2e\alpha_1] &= 0, \\
(\vec{x} \cdot \vec{z}) [-2a(1 - \alpha_4) + 2d(\alpha_4 - \alpha_5) + 2e\alpha_4] &= 0, \\
(\vec{y} \cdot \vec{z}) [-2a\alpha_1(1 - \alpha_4) - 2b(1 - \alpha_5) - 2d(1 - \alpha_1)(\alpha_4 - \alpha_5) + 2e\alpha_1\alpha_4 + 2f\alpha_5] &= 0.
\end{aligned} \tag{60}$$

Solving the equation in (60), for α_1, α_4 and α_5 gives

$$\alpha_1(a + d + e) = d, \implies \alpha_1 = \frac{d}{a + d + e}. \tag{61}$$

From the second line of Eq. (60),

$$\begin{aligned}
-(a + d + e)\alpha_4 &= -d\left(\alpha_5 + \frac{a}{d}\right), \\
\alpha_4 \equiv 1 - \alpha_2 &= \frac{d}{a + d + e}\left(\alpha_5 + \frac{a}{d}\right), \\
&= \alpha_1\left(\alpha_5 + \frac{a}{d}\right).
\end{aligned} \tag{62}$$

Using Eqs. (61) and (62) in Eq. (60) and solving for α_5 gives

$$\alpha_5 \equiv 1 - \alpha_3 = \frac{bd + 2\alpha_1 ad - \alpha_1^2 a(a + d + e)}{d(b + d + f - 2d\alpha_1 + \alpha_1^2(a + d + e))},$$

and using $a + d + e = \frac{d}{\alpha_1}$, we get

$$\begin{aligned}
\alpha_5 &= \frac{bd + 2\alpha_1 ad - \alpha_1 ad}{d(b + d + f - 2d\alpha_1 + \alpha_1 d)}, \\
&= \frac{\alpha_1 a + b}{(b + d + f - d\alpha_1)}.
\end{aligned} \tag{63}$$

Hence, from Eq. (59), we can write

$$\begin{aligned}
-ar_{12}^2 - \dots - fr_{34}^2 &= -a(x^2 + \alpha_1^2 y^2 + \alpha_2^2 z^2) - b(y^2 + \alpha_3^2 z^2) - cz^2 \\
&\quad - d(x^2 + (1 - \alpha_1)^2 y^2 + (\alpha_3 - \alpha_2)^2 z^2) \\
&\quad - e(x^2 + \alpha_1^2 y^2 + (1 - \alpha_2)^2 z^2) \\
&\quad - f(y^2 + (1 - \alpha_3)^2 z^2) \\
&= -x^2(a + d + e) - y^2(a\alpha_1^2 + b + d(1 - \alpha_1)^2 + e\alpha_1^2 + f) \\
&\quad - z^2(a\alpha_2^2 + b\alpha_3^2 + c + d(\alpha_3 - \alpha_2)^2 + e(1 - \alpha_2)^2 + f(1 - \alpha_3)^2).
\end{aligned} \tag{64}$$

It will be easy if we can simplify the different coefficients corresponding to x^2 , y^2 and z^2 one by one:

$$\begin{aligned}
x^2 : (a + d + e) &= \alpha_x \\
y^2 : (a\alpha_1^2 + b + d(1 - \alpha_1)^2 + e\alpha_1^2 + f) &= \alpha_1^2(a + d + e) + b + d + f - 2\alpha_1 d \\
&= \frac{d^2}{(a + d + e)^2} (a + d + e) + b + d + f - 2\frac{d^2}{(a + d + e)} \\
&= \frac{F_2(a, b, c, d, e, f)}{\alpha_x} \equiv \alpha_y \\
z^2 : (a\alpha_2^2 + b\alpha_3^2 + c + d(\alpha_3 - \alpha_2)^2 + e(1 - \alpha_2)^2 + f(1 - \alpha_3)^2) \\
&= (a(1 - \alpha_4)^2 + b(1 - \alpha_5)^2 + c + d(\alpha_4 - \alpha_5)^2 + e\alpha_4^2 + f\alpha_5^2) \\
&= (\alpha_4^2(a + d + e) + \alpha_5^2(b + d + f) + a + b + c - 2a\alpha_4 - 2b\alpha_5 - 2d\alpha_4\alpha_5) \\
&= \left(\alpha_1 \left(\alpha_5 + \frac{a}{d} \right)^2 d + \alpha_5^2 (b + d + f) + a + b + c - 2a\alpha_1 \left(\alpha_5 + \frac{a}{d} \right) - 2b\alpha_5 - 2d\alpha_1 \left(\alpha_5 + \frac{a}{d} \right) \alpha_5 \right) \\
&= \frac{F_1(a, b, c, d, e, f)}{F_2(a, b, c, d, e, f)} \equiv \alpha_z
\end{aligned} \tag{65}$$

where

$$\begin{aligned}
F_1(a, b, c, d, e, f) &= abc + abe + abf + acd + ade + acf + adf + aef \\
&\quad + bcd + bce + bde + bdf + bef + cde + cdf + cef,
\end{aligned} \tag{66}$$

and

$$\begin{aligned}
F_2(a, b, c, d, e, f) &= (b + d + f)(a + d + e) - d^2 \\
&= ab + ad + af + bd + be + de + df + ef.
\end{aligned} \tag{67}$$

Thus, the exponent of the Gaussian integral takes a simple form, which is

$$-ar_{12}^2 - \dots - fr_{34}^2 = -\alpha_x x^2 - \alpha_y y^2 - \alpha_z z^2. \tag{68}$$

In terms of eq. (68), we can write

$$\begin{aligned}
I(a, b, c, d, e, f) &= \int d^3\vec{r}_{12} d^3\vec{r}_{13} d^3\vec{r}_{14} \exp(-ar_{12}^2 - br_{13}^2 - cr_{14}^2 - dr_{23}^2 - er_{24}^2 - fr_{34}^2), \\
I(\alpha_x, \alpha_y, \alpha_z) &= \int d^3\vec{x} d^3\vec{y} d^3\vec{z} \exp(-\alpha_x x^2 - \alpha_y y^2 - \alpha_z z^2), \\
&= \int d^3\vec{x} \exp(-\alpha_x x^2) \int d^3\vec{y} \exp(-\alpha_y y^2) \int d^3\vec{z} \exp(-\alpha_z z^2), \\
I(\alpha_x, \alpha_y, \alpha_z) &= \frac{\pi^{9/2}}{(\alpha_x \alpha_y \alpha_z)^{3/2}} \because \int dx \exp(-\gamma x^2) = \frac{1}{2} \sqrt{\frac{\pi}{\gamma}}, \\
&= \frac{\pi^{9/2}}{[F_1(a, b, c, d, e, f)]^{3/2}}.
\end{aligned} \tag{69}$$

In fact, the expectation values of many other operators can be derived from $I(a, b, c, d, e, f)$ by using Feynman's parameters or parameter switch. We give $I(a, b, c, d, e, f)$ the name of the fundamental form regarding integration with ECG.

2.3.1 Overlap Integrals

The overlap matrix element S_{ij} reads

$$S_{ij} = \langle G_i^{1234} + G_j^{1234} | G_i^{1234} + G_j^{1234} \rangle \tag{70}$$

$$S_{ij} = \langle G_i^{1234} | G_i^{1234} \rangle + \langle G_i^{1234} | G_i^{1243} \rangle + \langle G_i^{1243} | G_i^{1234} \rangle + \langle G_i^{1243} | G_i^{1243} \rangle. \tag{71}$$

We see that each overlap matrix element is related to fundamental form of the integral $I(a, b, c, d, e, f)$,

$$\langle G_i^{1234} | G_i^{1234} \rangle = I(a, b, c, d, e, f), \quad (72)$$

$$\text{with } a = a_i + a_j, b = b_i + b_j, c = c_i + c_j, d = d_i + d_j, e = e_i + e_j, f = f_i + f_j. \quad (73)$$

$$\langle G_i^{1234} | G_i^{1243} \rangle = I(a, b, c, d, e, f), \quad (74)$$

$$\text{with } a = a_i + a_j, b = b_i + c_j, c = c_i + b_j, d = d_i + e_j, e = e_i + d_j, f = f_i + f_j. \quad (75)$$

$$\langle G_i^{1243} | G_i^{1234} \rangle = I(a, b, c, d, e, f), \quad (76)$$

$$\text{with } a = a_i + a_j, b = b_i + b_j, c = c_i + c_j, d = d_i + d_j, e = e_i + e_j, f = f_i + f_j. \quad (77)$$

$$\langle G_i^{1243} | G_i^{1243} \rangle = I(a, b, c, d, e, f), \quad (78)$$

$$\text{with } a = a_i + a_j, b = b_i + c_j, c = c_i + b_j, d = d_i + e_j, e = e_i + d_j, f = f_i + f_j. \quad (79)$$

2.3.2 Matrix Elements for Coulomb Potential

The Coulomb potential operator for PsH system is

$$\hat{V} = \frac{1}{r_{12}} + \frac{1}{r_{34}} - \frac{1}{r_{13}} - \frac{1}{r_{14}} - \frac{1}{r_{23}} - \frac{1}{r_{24}}. \quad (80)$$

Similar to the overlap matrix element, the Coulomb potential matrix element is

$$V_{ij} = \langle G_i^{1234} | \hat{V} G_i^{1234} \rangle + \langle G_i^{1234} | \hat{V} G_i^{1243} \rangle + \langle G_i^{1243} | \hat{V} G_i^{1234} \rangle + \langle G_i^{1243} | \hat{V} G_i^{1243} \rangle. \quad (81)$$

Again, those four terms have the exact same the format as in eq. (72-78). Given the choice of coordinate shift, eq. (57), we can directly solve for the potential integral V_{14} ,

$$V_{14}(a, b, c, d, e, f) = \int d^3\vec{r}_{12}d^3\vec{r}_{13}d^3\vec{r}_{14}\frac{1}{r_{14}} \exp(-ar_{12}^2 - br_{13}^2 - cr_{14}^2 - dr_{23}^2 - er_{24}^2 - fr_{34}^2) \quad (82)$$

$$= \frac{\pi^3}{(\alpha_x\alpha_y)^{3/2}} \int d^3\vec{z}\frac{1}{z}e^{-\alpha_z z^2} \quad (83)$$

$$= \frac{2\pi^{9/2}}{\sqrt{\pi}F_1(a, b, c, d, e, f) [F_2(a, b, c, d, e, f)]^{1/2}} \quad (84)$$

The other Coulomb integrals can be easily calculated by swapping the parameters. For example,

$$V_{12}(a, b, c, d, e, f) = \int d^3\vec{r}_{12}d^3\vec{r}_{13}d^3\vec{r}_{14}\left(\frac{1}{r_{12}}\right) \exp(-ar_{12}^2 - br_{13}^2 - cr_{14}^2 - dr_{23}^2 - er_{24}^2 - fr_{34}^2) \quad (85)$$

$$= \int d^3\vec{r}_{14}d^3\vec{r}_{13}d^3\vec{r}_{12}\left(\frac{1}{r_{12}}\right) \exp(-cr_{14}^2 - br_{13}^2 - ar_{12}^2 - fr_{34}^2 - er_{24}^2 - dr_{23}^2) \quad (86)$$

$$= \int d^3\vec{r}_{14}d^3\vec{r}_{13}d^3\vec{r}_{12}\left(\frac{1}{r_{14}}\right) \exp(-cr_{12}^2 - br_{13}^2 - ar_{14}^2 - fr_{23}^2 - er_{24}^2 - dr_{34}^2) \quad (87)$$

$$= V_{14}(c, b, a, f, e, d). \quad (88)$$

We first rearrange our integral so that \vec{r}_{12} has the same effect as \vec{r}_{14} , then we swap $\{2 \leftrightarrow 4\}$ to arrive at the final result.

Similarly,

$$V_{13}(a, b, c, d, e, f) = V_{14}(a, c, b, e, d, f)$$

$$V_{23}(a, b, c, d, e, f) = V_{14}(a, e, d, c, b, f)$$

$$V_{24}(a, b, c, d, e, f) = V_{14}(a, d, e, b, c, f)$$

$$V_{34}(a, b, c, d, e, f) = V_{14}(b, d, f, a, c, e)$$

2.3.2.1 Kinetic energy

We have the kinetic energy operator for the PsH system,

$$\hat{T} = -\frac{1}{2\mu_{12}} \left[\vec{\nabla}_{\vec{r}_{12}}^2 + \vec{\nabla}_{\vec{r}_{13}}^2 + \vec{\nabla}_{\vec{r}_{14}}^2 \right] - \frac{1}{m_1} \left[\vec{\nabla}_{\vec{r}_{12}} \cdot \vec{\nabla}_{\vec{r}_{13}} + \vec{\nabla}_{\vec{r}_{12}} \cdot \vec{\nabla}_{\vec{r}_{14}} + \vec{\nabla}_{\vec{r}_{13}} \cdot \vec{\nabla}_{\vec{r}_{14}} \right]$$

The gradient operator is acting on the inter-particle distances. The six inter-particle displacement in the ECGs basis are not independent. In fact

$$\begin{aligned}\vec{r}_{23} &= \vec{r}_{13} - \vec{r}_{12} \\ \vec{r}_{24} &= \vec{r}_{14} - \vec{r}_{12} \\ \vec{r}_{34} &= \vec{r}_{14} - \vec{r}_{13}\end{aligned}$$

From the law of cosines

$$\begin{aligned}r_{23}^2 &= r_{12}^2 + r_{13}^2 - 2\vec{r}_{12} \cdot \vec{r}_{13}, \\ r_{24}^2 &= r_{12}^2 + r_{14}^2 - 2\vec{r}_{12} \cdot \vec{r}_{14}, \\ r_{34}^2 &= r_{13}^2 + r_{14}^2 - 2\vec{r}_{13} \cdot \vec{r}_{14}\end{aligned}\tag{89}$$

Consider the gradient acting on the basis function

$$\begin{aligned}\nabla_{\vec{r}_{12}} |G_i^{1234}\rangle &= [-2(a_i + d_i + e_i)\vec{r}_{12} + 2d_i\vec{r}_{13} + 2e_i\vec{r}_{14}] |G_i^{1234}\rangle \\ \nabla_{\vec{r}_{13}} |G_i^{1234}\rangle &= [-2(b_i + d_i + f_i)\vec{r}_{13} + 2d_i\vec{r}_{12} + 2f_i\vec{r}_{14}] |G_i^{1234}\rangle \\ \nabla_{\vec{r}_{14}} |G_i^{1234}\rangle &= [-2(c_i + e_i + f_i)\vec{r}_{14} + 2e_i\vec{r}_{12} + 2f_i\vec{r}_{13}] |G_i^{1234}\rangle.\end{aligned}\tag{90}$$

The following gradient identities are used in eq. (90),

$$\begin{aligned}\frac{\partial r_k}{\partial r_j} &= \delta_{kj}, \\ \frac{\partial}{\partial r_1^j} r_1^2 &= \frac{\partial}{\partial r_1^j} (r_1^k r_1^k) = 2r_1^k \delta^{jk} = 2r_1^j \\ \frac{\partial}{\partial r_1^j} (r_1 \cdot r_2) &= \frac{\partial}{\partial r_1^j} (r_1^k r_2^k) = \delta^{jk} r_2^k = r_2^j.\end{aligned}\tag{91}$$

The dimension of the inter-particle displacement vector is 3. The second order differential operator for all term is calculated as (we use $\delta_{ii} = 3$)

$$\begin{aligned}
\nabla_{\vec{r}_{12}}^2 |\psi_i^{1234}\rangle &= \vec{\nabla}_{\vec{r}_{12}} \cdot \vec{\nabla}_{\vec{r}_{12}} |\psi_i^{1234}\rangle, \\
&= \vec{\nabla}_{\vec{r}_{12}} \cdot [(-2(a_i + d_i + e_i)\vec{r}_{12} + 2d_i\vec{r}_{13} + 2e_i\vec{r}_{14}) |\psi_i^{1234}\rangle], \\
&= -6(a_i + d_i + e_i) |\psi_i^{1234}\rangle + [-2(a_i + d_i + e_i)\vec{r}_{12} + 2d_i\vec{r}_{13} + 2e_i\vec{r}_{14}] \cdot \vec{\nabla}_{\vec{r}_{12}} |\psi_i^{1234}\rangle, \\
&= -6(a_i + d_i + e_i) |\psi_i^{1234}\rangle + [-2(a_i + d_i + e_i)\vec{r}_{12} + 2d_i\vec{r}_{13} + 2e_i\vec{r}_{14}] \cdot \\
&\quad [-2(a_i + d_i + e_i)\vec{r}_{12} + 2d_i\vec{r}_{13} + 2e_i\vec{r}_{14}] |\psi_i^{1234}\rangle \\
&= -6(a_i + d_i + e_i) |\psi_i^{1234}\rangle + 4 \left[(a_i + d_i + e_i)^2 r_{12}^2 + d_i^2 r_{13}^2 + e_i^2 r_{14}^2 - 2d_i(a_i + d_i + e_i)\vec{r}_{12} \cdot \vec{r}_{13} \right. \\
&\quad \left. - 2e_i(a_i + d_i + e_i)\vec{r}_{12} \cdot \vec{r}_{14} + 2d_i e_i \vec{r}_{13} \cdot \vec{r}_{14} \right] |\psi_i^{1234}\rangle,
\end{aligned} \tag{92}$$

$$\begin{aligned}
\nabla_{\vec{r}_{13}}^2 |\psi_i^{1234}\rangle &= \vec{\nabla}_{\vec{r}_{13}} \cdot [(-2(b_i + d_i + f_i)\vec{r}_{13} + 2d_i\vec{r}_{12} + 2f_i\vec{r}_{14}) |\psi_i^{1234}\rangle], \\
&= -6(b_i + d_i + f_i) |\psi_i^{1234}\rangle + 4 \left[(b_i + d_i + f_i)^2 r_{13}^2 + d_i^2 r_{12}^2 + f_i^2 r_{14}^2 - 2d_i(b_i + d_i + f_i)\vec{r}_{12} \cdot \vec{r}_{13} \right. \\
&\quad \left. - 2f_i(b_i + d_i + f_i)\vec{r}_{13} \cdot \vec{r}_{14} + 2d_i f_i \vec{r}_{12} \cdot \vec{r}_{14} \right] |\psi_i^{1234}\rangle,
\end{aligned} \tag{93}$$

$$\begin{aligned}
\nabla_{\vec{r}_{14}}^2 |\psi_i^{1234}\rangle &= -6(c_i + e_i + f_i) |\psi_i^{1234}\rangle + [(-2(c_i + e_i + f_i)\vec{r}_{14} + 2e_i\vec{r}_{12} + 2f_i\vec{r}_{13}) \cdot \\
&\quad (-2(c_i + e_i + f_i)\vec{r}_{14} + 2e_i\vec{r}_{12} + 2f_i\vec{r}_{13})] |\psi_i^{1234}\rangle \\
&= -6(c_i + e_i + f_i) |\psi_i^{1234}\rangle + 4 \left[(c_i + e_i + f_i)^2 r_{14}^2 + e_i^2 r_{12}^2 + f_i^2 r_{13}^2 - 2e_i(c_i + e_i + f_i)\vec{r}_{12} \cdot \vec{r}_{14} \right. \\
&\quad \left. - 2f_i(c_i + e_i + f_i)\vec{r}_{13} \cdot \vec{r}_{14} + 2e_i f_i \vec{r}_{12} \cdot \vec{r}_{13} \right] |\psi_i^{1234}\rangle.
\end{aligned} \tag{94}$$

$$\begin{aligned}
\vec{\nabla}_{\vec{r}_{12}} \cdot \vec{\nabla}_{\vec{r}_{13}} |\psi_i^{1234}\rangle &= \vec{\nabla}_{\vec{r}_{12}} \cdot [(-2(b_i + d_i + f_i) \vec{r}_{13} + 2d_i \vec{r}_{12} + 2f_i \vec{r}_{14}) |\psi_i^{1234}\rangle] \\
&= \left[6d_i + (-2(b_i + d_i + f_i) \vec{r}_{13} + 2d_i \vec{r}_{12} + 2f_i \vec{r}_{14}) \right. \\
&\quad \left. \cdot (-2(a_i + d_i + e_i) \vec{r}_{12} + 2d_i \vec{r}_{13} + 2e_i \vec{r}_{14}) \right] |\psi_i^{1234}\rangle \tag{95}
\end{aligned}$$

$$\begin{aligned}
&= [6d_i + 4[-d_i(a_i + d_i + e_i)r_{12}^2 - d_i(b_i + d_i + f_i)r_{13}^2 + e_i f_i r_{14}^2 \\
&\quad [d_i^2 + (b_i + d_i + f_i)(a_i + d_i + e_i)] \vec{r}_{12} \cdot \vec{r}_{13} + [d_i f_i - e_i(b_i + d_i + f_i)] \vec{r}_{13} \cdot \vec{r}_{14} \\
&\quad [d_i e_i - f_i(a_i + d_i + e_i)] \vec{r}_{12} \cdot \vec{r}_{14}] |\psi_i^{1234}\rangle. \tag{96}
\end{aligned}$$

$$\begin{aligned}
\vec{\nabla}_{\vec{r}_{12}} \cdot \vec{\nabla}_{\vec{r}_{14}} |\psi_i^{1234}\rangle &= \vec{\nabla}_{\vec{r}_{12}} \cdot [(-2(c_i + e_i + f_i) \vec{r}_{14} + 2e_i \vec{r}_{12} + 2f_i \vec{r}_{13}) |\psi_i^{1234}\rangle] \\
&= \left[6e_i + (-2(c_i + e_i + f_i) \vec{r}_{14} + 2e_i \vec{r}_{12} + 2f_i \vec{r}_{13}) \right. \\
&\quad \left. \cdot (-2(a_i + d_i + e_i) \vec{r}_{12} + 2d_i \vec{r}_{13} + 2e_i \vec{r}_{14}) \right] |\psi_i^{1234}\rangle \tag{97}
\end{aligned}$$

$$\begin{aligned}
&= [6e_i + 4[-e_i(a_i + d_i + e_i)r_{12}^2 + d_i f_i r_{13}^2 - e_i(c_i + e_i + f_i)r_{14}^2 \\
&\quad [d_i e_i - f_i(a_i + d_i + e_i)] \vec{r}_{12} \cdot \vec{r}_{13} + [e_i f_i - d_i(c_i + e_i + f_i)] \vec{r}_{13} \cdot \vec{r}_{14} \\
&\quad [e_i^2 + (a_i + d_i + e_i)(c_i + e_i + f_i)] \vec{r}_{12} \cdot \vec{r}_{14}] |\psi_i^{1234}\rangle. \tag{98}
\end{aligned}$$

$$\begin{aligned}
\vec{\nabla}_{\vec{r}_{13}} \cdot \vec{\nabla}_{\vec{r}_{14}} |\psi_i^{1234}\rangle &= \vec{\nabla}_{\vec{r}_{13}} \cdot [(-2(c_i + e_i + f_i) \vec{r}_{14} + 2e_i \vec{r}_{12} + 2f_i \vec{r}_{13}) |\psi_i^{1234}\rangle] \\
&= [6f_i + (-2(c_i + e_i + f_i) \vec{r}_{14} + 2e_i \vec{r}_{12} + 2f_i \vec{r}_{13}) \\
&\quad \cdot (-2(b_i + d_i + f_i) \vec{r}_{13} + 2d_i \vec{r}_{12} + 2f_i \vec{r}_{14})] |\psi_i^{1234}\rangle \tag{99}
\end{aligned}$$

$$\begin{aligned}
&= [6f_i + 4[d_i e_i r_{12}^2 - f_i(b_i + d_i + f_i)r_{13}^2 - f_i(c_i + e_i + f_i)r_{14}^2 \\
&\quad [d_i f_i - e_i(b_i + d_i + f_i)] \vec{r}_{12} \cdot \vec{r}_{13} + [f_i^2 + (b_i + d_i + f_i)(c_i + e_i + f_i)] \vec{r}_{13} \cdot \vec{r}_{14} \\
&\quad [e_i f_i - d_i(c_i + e_i + f_i)] \vec{r}_{12} \cdot \vec{r}_{14}] |\psi_i^{1234}\rangle. \tag{100}
\end{aligned}$$

We use eq. (89) and collect terms with the same order of inter-particle distances r_{ij}^n .

Constant Terms: $|G_i^{1234}\rangle$

$$\begin{aligned}
& -\frac{1}{2\mu_{12}} [-6(a_i + d_i + e_i) - 6(b_i + d_i + f_i) - 6(c_i + e_i + f_i)] - \frac{1}{m_1} [6d_i + 6e_i + 6f_i] \\
& = -\frac{1}{2\mu_{12}} [-6(a_i + b_i + c_i + 2d_i + 2e_i + 2f_i)] - \frac{1}{m_1} [6(d_i + e_i + f_i)] \\
& = \frac{3}{\mu_{12}} (a_i + b_i + c_i + 2d_i + 2e_i + 2f_i) - \frac{6}{m_1} (d_i + e_i + f_i).
\end{aligned} \tag{101}$$

r_{12}^2 Terms: $r_{12}^2 |G_i^{1234}\rangle$

$$-\frac{2}{\mu_{12}} (a_i^2 + a_i d_i - b_i d_i + a_i e_i - c_i e_i) - \frac{2}{m_1} (a_i b_i + a_i c_i - a_i d_i + b_i d_i - a_i e_i + c_i e_i).$$

r_{13}^2 Terms: $r_{13}^2 |G_i^{1234}\rangle$

$$-\frac{2}{\mu_{12}} (b_i^2 - a_i d_i + b_i d_i + b_i f_i - c_i f_i) - \frac{2}{m_1} (a_i b_i + b_i c_i + a_i d_i - b_i d_i - b_i f_i + c_i f_i).$$

r_{14}^2 Terms: $r_{14}^2 |G_i^{1234}\rangle$

$$-\frac{2}{\mu_{12}} (c_i^2 - a_i e_i + c_i e_i - b_i f_i + c_i f_i) - \frac{2}{m_1} (a_i c_i + b_i c_i + a_i e_i - c_i e_i + b_i f_i - c_i f_i).$$

r_{23}^2 Terms: $r_{23}^2 |G_i^{1234}\rangle$

$$-\frac{2}{\mu_{12}} (2d_i^2 + a_i d_i + b_i d_i + d_i e_i + d_i f_i - e_i f_i) + \frac{2}{m_1} (2d_i^2 + a_i b_i + a_i d_i + b_i d_i + d_i e_i + d_i f_i - e_i f_i).$$

r_{24}^2 Terms: $r_{24}^2 |G_i^{1234}\rangle$

$$-\frac{2}{\mu_{12}} (2e_i^2 + a_i e_i + c_i e_i + d_i e_i - d_i f_i - e_i f_i) + \frac{2}{m_1} (2e_i^2 + a_i c_i + a_i e_i + c_i e_i + d_i e_i - d_i f_i - e_i f_i).$$

r_{34}^2 Terms: $r_{34}^2 |G_i^{1234}\rangle$

$$-\frac{2}{\mu_{12}} (2f_i^2 - d_i e_i + b_i f_i + c_i f_i + d_i f_i + e_i f_i) + \frac{2}{m_1} (2f_i^2 + b_i c_i - d_i e_i + b_i f_i + c_i f_i + d_i f_i + e_i f_i).$$

Finally, the matrix element for the kinetic energy operator is

$$\begin{aligned} \langle \psi_i^{1234} | \hat{T} | \psi_j^{1234} \rangle &= \left[\frac{3}{\mu_{12}} (a_i + b_i + c_i + 2d_i + 2e_i + 2f_i) - \frac{6}{m_1} (d_i + e_i + f_i) \right] \langle \psi_i^{1234} | \psi_j^{1234} \rangle \\ &- 2 \left[\frac{1}{\mu_{12}} (a_i^2 + a_i d_i - b_i d_i + a_i e_i - c_i e_i) + \frac{1}{m_1} (a_i b_i + a_i c_i - a_i d_i + b_i d_i - a_i e_i + c_i e_i) \right] \\ &\cdot \langle r_{12}^2 \rangle \end{aligned} \quad (102)$$

$$\begin{aligned} &- 2 \left[\frac{1}{\mu_{12}} (b_i^2 - a_i d_i + b_i d_i + b_i f_i - c_i f_i) + \frac{1}{m_1} (a_i b_i + b_i c_i + a_i d_i - b_i d_i - b_i f_i + c_i f_i) \right] \\ &\cdot \langle r_{13}^2 \rangle \end{aligned} \quad (103)$$

$$\begin{aligned} &- 2 \left[\frac{1}{\mu_{12}} (c_i^2 - a_i e_i + c_i e_i - b_i f_i + c_i f_i) + \frac{1}{m_1} (a_i c_i + b_i c_i + a_i e_i - c_i e_i + b_i f_i - c_i f_i) \right] \\ &\cdot \langle r_{14}^2 \rangle \end{aligned} \quad (104)$$

$$\begin{aligned} &- 2 \left[\frac{1}{\mu_{12}} (2d_i^2 + a_i d_i + b_i d_i + d_i e_i + d_i f_i - e_i f_i) \right. \\ &- \left. \frac{1}{m_1} (2d_i^2 + a_i b_i + a_i d_i + b_i d_i + d_i e_i + d_i f_i - e_i f_i) \right] \langle r_{23}^2 \rangle \\ &- 2 \left[\frac{1}{\mu_{12}} (2e_i^2 + a_i e_i + c_i e_i + d_i e_i - d_i f_i + e_i f_i) \right. \\ &- \left. \frac{1}{m_1} (2e_i^2 + a_i c_i + a_i e_i + c_i e_i + d_i e_i - d_i f_i + e_i f_i) \right] \langle r_{24}^2 \rangle \\ &- 2 \left[\frac{1}{\mu_{12}} (2f_i^2 - d_i e_i + b_i f_i + c_i f_i + d_i f_i + e_i f_i) \right. \\ &- \left. \frac{1}{m_1} (2f_i^2 + b_i c_i - d_i e_i + b_i f_i + c_i f_i + d_i f_i + e_i f_i) \right] \langle r_{34}^2 \rangle, \end{aligned} \quad (105)$$

where $\langle r_{ij}^2 \rangle = \langle \psi^{1234} | r_{ij}^2 | \psi^{1234} \rangle$ are the expectation values of the square of inter-particle distances. In order to calculate them, first consider

$$\langle r_{14}^2 \rangle (a, b, c, d, e, f) = \int d^3 \vec{r}_{12} d^3 \vec{r}_{13} d^3 \vec{r}_{14} (r_{14}^2) \exp(-ar_{12}^2 - br_{13}^2 - cr_{14}^2 - dr_{23}^2 - er_{24}^2 - fr_{34}^2), \quad (106)$$

which in terms of $(\vec{x}, \vec{y}, \vec{z})$ and following the procedure of Eq. (69), become

$$\begin{aligned}
\langle r_{14}^2 \rangle (a, b, c, d, e, f) &= \int d^3 \vec{x} d^3 \vec{y} d^3 \vec{z} (z^2) \exp(-\alpha_x x^2 - \alpha_y y^2 - \alpha_z z^2) \\
&= \frac{\pi^3}{(\alpha_x \alpha_y)^{3/2}} \int d^3 \vec{z} (z^2) \exp(-\alpha_z z^2) \\
&= \frac{4\pi^4}{(\alpha_x \alpha_y)^{3/2}} \int dz z^4 \exp(-\alpha_z z^2).
\end{aligned} \tag{107}$$

We know that

$$\begin{aligned}
\int dx e^{-ax^2} &= \frac{1}{2} \sqrt{\frac{\pi}{a}} \\
\frac{d}{da} \int dx e^{-ax^2} &= \int dx x^2 e^{-ax^2} = \frac{1}{4} \frac{\sqrt{\pi}}{a^{3/2}} \\
\frac{d}{da} \int dx x^2 e^{-ax^2} &= \int dx x^4 e^{-ax^2} = \frac{3}{8} \frac{\sqrt{\pi}}{a^{5/2}}.
\end{aligned} \tag{108}$$

Thus

$$\begin{aligned}
\langle r_{14}^2 \rangle (a, b, c, d, e, f) &= \frac{4\pi^4}{(\alpha_x \alpha_y)^{3/2}} \frac{3}{8} \frac{\sqrt{\pi}}{\alpha_z^{5/2}} \\
&= \frac{3\pi^{9/2}}{2\alpha_z (\alpha_x \alpha_y \alpha_z)^{3/2}} \\
&= \frac{3\pi^{9/2} F_2(a, b, c, d, e, f)}{2 (F_1(a, b, c, d, e, f))^{5/2}}
\end{aligned} \tag{109}$$

where a, \dots, f are given in Eq. (69).

$$\begin{aligned}
\langle r_{12}^2 \rangle (\mathbf{a}, b, \mathbf{c}, \mathbf{d}, e, \mathbf{f}) &= \langle r_{14}^2 \rangle (\mathbf{c}, b, \mathbf{a}, \mathbf{f}, e, \mathbf{d}), \\
\langle r_{13}^2 \rangle (a, \mathbf{b}, \mathbf{c}, \mathbf{d}, e, f) &= \langle r_{14}^2 \rangle (a, \mathbf{c}, \mathbf{b}, \mathbf{e}, \mathbf{d}, f), \\
\langle r_{23}^2 \rangle (a, \mathbf{b}, \mathbf{c}, \mathbf{d}, e, f) &= \langle r_{14}^2 \rangle (a, \mathbf{e}, \mathbf{d}, \mathbf{c}, \mathbf{b}, f), \\
\langle r_{24}^2 \rangle (a, \mathbf{b}, \mathbf{c}, \mathbf{d}, e, f) &= \langle r_{14}^2 \rangle (a, \mathbf{d}, \mathbf{e}, \mathbf{b}, \mathbf{c}, f), \\
\langle r_{34}^2 \rangle (\mathbf{a}, \mathbf{b}, \mathbf{c}, \mathbf{d}, e, \mathbf{f}) &= \langle r_{14}^2 \rangle (\mathbf{b}, \mathbf{d}, \mathbf{f}, \mathbf{a}, \mathbf{c}, \mathbf{e}).
\end{aligned} \tag{110}$$

2.3.2.2 Inverse Square of Inter-particle distances

Here we will calculate the matrix elements for the inverse square of the inter-particle distances, i.e., the matrix elements of the type $\langle \psi_j^{1234} | \frac{1}{r_{ab}^2} | \psi_i^{1234} \rangle$. With the method used above, we get

$$\langle \psi_j^{1234} | \frac{1}{r_{14}^2} | \psi_i^{1234} \rangle = \int d^3 \vec{r}_{12} d^3 \vec{r}_{13} d^3 \vec{r}_{14} (r_{14}^2) \exp(-ar_{12}^2 - br_{13}^2 - cr_{14}^2 - dr_{23}^2 - er_{24}^2 - fr_{34}^2),$$

which in terms of $(\vec{x}, \vec{y}, \vec{z})$ and following Eq. (69) becomes

$$\begin{aligned} \left\langle \frac{1}{r_{14}^2} \right\rangle (a, b, c, d, e, f) &= \int d^3 \vec{x} d^3 \vec{y} d^3 \vec{z} \left(\frac{1}{z^2} \right) \exp(-\alpha_x x^2 - \alpha_y y^2 - \alpha_z z^2) \\ &= \frac{4\pi^4}{(\alpha_x \alpha_y)^{3/2}} \int dz \exp(-\alpha_z z^2) \\ &= \frac{2\pi^{9/2}}{F_2(a, b, c, d, e, f) [F_1(a, b, c, d, e, f)]^{1/2}}. \end{aligned} \quad (111)$$

Likewise, the other needed quantities can be expressed in terms of above matrix elements as

$$\begin{aligned} \left\langle \frac{1}{r_{12}^2} \right\rangle (a, b, c, d, e, f) &= \left\langle \frac{1}{r_{14}^2} \right\rangle (c, b, a, f, e, d), \\ \left\langle \frac{1}{r_{13}^2} \right\rangle (a, b, c, d, e, f) &= \left\langle \frac{1}{r_{14}^2} \right\rangle (a, c, b, e, d, f), \\ \left\langle \frac{1}{r_{23}^2} \right\rangle (a, b, c, d, e, f) &= \left\langle \frac{1}{r_{14}^2} \right\rangle (a, e, d, c, b, f), \\ \left\langle \frac{1}{r_{24}^2} \right\rangle (a, b, c, d, e, f) &= \left\langle \frac{1}{r_{14}^2} \right\rangle (a, d, e, b, c, f), \\ \left\langle \frac{1}{r_{34}^2} \right\rangle (a, b, c, d, e, f) &= \left\langle \frac{1}{r_{14}^2} \right\rangle (b, d, f, a, c, e). \end{aligned} \quad (112)$$

The definition of a, \dots, f is given in Eq. (72 - 78). The matrix elements for the other states can be calculated in a similar fashion to exhaust all the permutations by swapping the parameters.

2.3.2.3 Inter Particle Distances

In order to calculate the inter particle distances, we have to calculate the matrix elements of the type

$$\langle r_{ab} \rangle = \langle \psi_j^{1234} | \hat{r}_{ab} | \psi_i^{1234} \rangle.$$

Again, we will start with r_{14} and write the others in terms of it

$$\begin{aligned}
\langle r_{14} \rangle &= \langle \psi_j^{1234} | \hat{r}_{14} | \psi_i^{1234} \rangle \\
&= \int d^3 \vec{r}_{12} d^3 \vec{r}_{13} d^3 \vec{r}_{14} r_{14} \exp(-ar_{12}^2 - br_{13}^2 - cr_{14}^2 - dr_{23}^2 - er_{24}^2 - fr_{34}^2), \\
&= \int d^3 \vec{x} \exp(-\alpha_x x^2) \int d^3 \vec{y} \exp(-\alpha_y y^2) \int d^3 \vec{z}(z) \exp(-\alpha_z z^2), \\
&= 2\pi^{9/2} \frac{[F_2(a, b, c, d, e, f)]^{1/2}}{\sqrt{\pi} [F_1(a, b, c, d, e, f)]^2} \equiv \langle r_{14} \rangle(a, b, c, d, e, f).
\end{aligned} \tag{113}$$

With the scheme used in the calculation of potential energy, we get

$$\begin{aligned}
\langle r_{12} \rangle(a, b, c, d, e, f) &= \langle r_{14} \rangle(c, b, a, f, e, d), \\
\langle r_{13} \rangle(a, b, c, d, e, f) &= \langle r_{14} \rangle(a, c, b, e, d, f), \\
\langle r_{23} \rangle(a, b, c, d, e, f) &= \langle r_{14} \rangle(a, e, d, c, b, f), \\
\langle r_{24} \rangle(a, b, c, d, e, f) &= \langle r_{14} \rangle(a, d, e, b, c, f), \\
\langle r_{34} \rangle(a, b, c, d, e, f) &= \langle r_{14} \rangle(b, d, f, a, c, e).
\end{aligned} \tag{114}$$

2.3.3 Numerical Evaluation

In order to perform the numerical calculation using variational approach, a code developed by Puchalski and Czarnecki [14], whose structure is described in the Appendix, is used to optimize values of the parameters. The code is run until the time the basis size reaches 1000. However, if necessary, in future the calculation can be extended to improve accuracy. Numerical values of the expectation values of different parameters of PsH are given in Table 2.

By looking at the value of the inter-particle distances in the PsH, we can see that this molecule is slightly more extended than the ordinary positronium atom with relative electron-positron distances ($\langle r_{e-e^+} \rangle$) to be $3.48a_0$ and $3.0a_0$, respectively. The average distance of electrons from the proton ($\langle r_{e-p} \rangle$) is $2.31a_0$ which is larger than the dihydrogen. The average distance between positron-proton ($\langle r_{e^+p} \rangle$) is $3.66a_0$ which is much larger than $1.41a_0$ that is the average distance between two protons ($\langle r_{pp} \rangle$) in the H_2 . We see from Table 2 that these values agree with the one obtained in ref. [2].

Table 2: Expectation values of parameters of PsH and their comparison with [2]. In our work, we compared the values by taking both the 100 and 1000 basis.

Property	Mitroy [2]	Ours	Ours
N	1800	100	1000
$\langle V \rangle / \langle T \rangle + 2$	7.3×10^{-8}	2.0×10^{-5}	-1.1×10^{-6}
E	-0.788870618	-0.788777722	-0.7888702781
$\langle T_- \rangle$	0.3261733	0.3258211	0.32585599
$\langle T_+ \rangle$	0.1368503	0.1368260	0.13683160
$\langle r_{H^+e^-} \rangle$	2.311526	2.3105613	2.31314158
$\langle r_{H^+e^+} \rangle$	3.661624	3.6587151	3.66346165
$\langle r_{e^-e^-} \rangle$	3.574787	3.5718503	3.57698395
$\langle r_{e^+e^-} \rangle$	3.480272	3.4782961	3.48115262
$\langle 1/r_{H^+e^-} \rangle$	0.7297090	0.7293035	0.7292580
$\langle 1/r_{H^+e^+} \rangle$	0.3474618	0.3474887	0.3473026
$\langle 1/r_{e^-e^-} \rangle$	0.3705549	0.3704987	0.37033136
$\langle 1/r_{e^+e^-} \rangle$	0.4184961	0.41847598	0.4184289
$\langle r_{H^+e^-}^2 \rangle$	7.813046	7.78840188	7.8244646
$\langle r_{H^+e^+}^2 \rangle$	16.25453	16.2021879	16.271458
$\langle r_{e^-e^-}^2 \rangle$	15.87546	15.8193644	15.895276
$\langle r_{e^+e^-}^2 \rangle$	15.58427	15.5482392	15.593128
$\langle 1/r_{H^+e^-}^2 \rangle$	1.207067	1.20451062	1.2056154
$\langle 1/r_{H^+e^+}^2 \rangle$	0.1721631	0.1723848	0.1720162
$\langle 1/r_{e^-e^-}^2 \rangle$	0.2139099	0.2138301	0.21364909
$\langle 1/r_{e^+e^-}^2 \rangle$	0.3491440	0.3487406	0.34906742

The binding energy (also known as the dissociation energy) is given by

$$\begin{aligned}
 E_b &= -E_1 + E_1^H + E_1^{\text{Ps}} \\
 &= -E_1 - \frac{3}{4} \text{a.u.}
 \end{aligned} \tag{115}$$

where the ground state energies of hydrogen and positronium are $-\frac{1}{2}$ a.u. and $-\frac{1}{4}$ a.u., respectively. (a.u. denotes atomic units also called hartree.) From Table 1 we see that with $E_1 = -0.788\ 870\ 345\ 206$ hartree the PsH forms a stable structure with respect to auto-dissociation.

The numerical values of the other parameter of the PsH is summarized in Table 2 where $\langle r_{ij} \rangle$ represent the expectation values of the inter-particle distances, $\langle 1/r_{ij} \rangle$ the inverse of that, and the positron and electron kinetic energy operators are written as T_+ and T_- , respectively. These values agree well with the corresponding one obtained in [2].

Chapter 3

Stability of Tetrons

A recent revival of the interest in tetrons is inspired by the observation [61] by LHCb of a double charmed baryon $\Xi_{cc}^{++} \sim ccu$. The measurement of the mass of the baryon at about 3621 MeV has provided an estimate of the effective mass of the heavy quark pair cc (with the interaction between the quarks in the color anti-triplet state), and thus an input into phenomenological models [62, 63].

The latter models are based on the picture [11] where, due to the attraction in the color-antisymmetric state, the heavy quark pair forms a compact, in fact a point-like, bound state. This bound state then acts essentially as a heavy antiquark and binds either with a light quark to form a baryon, e.g. Ξ_{cc}^{++} , or with a light antiquark pair to form a tetron, e.g. $Q_a Q_b \bar{u} \bar{d}$. Since the latter binding is similar to that in respectively a heavy meson and a heavy (anti)baryon, by applying the known mass differences, e.g. between Λ_c and D , or between Λ_b and the B -meson, the masses of possible tetrons containing cc , or bb , or bc heavy quark pair can be estimated. In this way it has been argued [62, 63] that there are no stable tetrons with cc heavy quark pair, but there definitely is a $bb\bar{u}\bar{d}$ one, well below the $B^- \bar{B}^0$ threshold, and also likely similar weakly decaying strange tetrons [63] $bb\bar{s}\bar{q}$ with q standing for either u or d . (The conclusion about existence of mixed bottom-charm tetrons $bc\bar{q}\bar{q}$ is uncertain in Ref.[62] and negative in [63].) Numerical evidence for such states has been established in lattice nonrelativistic QCD [64], as well as using the approximation of static b -quarks [65].

It is clear however that the similarity of the interaction in a tetron to that in an (anti)baryon, where a heavy antiquark is replaced by a compact color-antisymmetric pair of heavy quarks is not exact. One simple reason for a deviation is the spin-dependent interaction, which is suppressed for heavy quarks and which to some extent can be accounted for [63]. The other (and less tractable) reason is that the heavy quark pair has a finite size with the most important effect being a flip of the color state from antisymmetric to symmetric (with the corresponding change of the color of the light antiquark pair). The existence of these configuration was recognized in the previous studies [12, 66, 67] and was taken into account in a series of approximations.

In what follows we treat the mixing of the color configurations explicitly within an expansion in the ratio of the distance between the heavy quarks to the characteristic distance to the light antiquarks. The point-like

limit [11, 62, 63] is the first term in this expansion. It naturally appears that for sufficiently heavy quark pair with the (reduced) mass M , the characteristic size of the bound state is proportional to $1/M$, while the distance scale for the light (massless) antiquarks in a tetron is set by Λ_{QCD} , so that the ratio of the distance scales is proportional to Λ_{QCD}/M . We will argue however that the effects of the deviation from the point-like approximation are enhanced in the limit of large number N_c of colors, so that the relevant parameter for this deviation is in fact

$$\xi = N_c^6 \left(\frac{\Lambda_{QCD}}{M} \right)^4 \quad (116)$$

which at $N_c = 3$ indicates that the point-like limit is not applicable if at least one of the heavy quarks is the charmed one. On the other hand, this limit may work with reasonably small corrections of order ξ for tetrons with the $b\bar{b}$ quark pair.

Furthermore, it appears that a stable tetron does not exist if the parameter ξ is of order one or larger. To establish this behavior, we consider in Section 3.4 the limit where all the quarks and the antiquarks are asymptotically heavy, so that the relevant distances for bound states are short. One can then apply the Coulomb-like limit for the gluon exchange among all constituents, with a non-relativistic Hamiltonian describing the interplay of color configurations. The two scales are introduced in this model by considering the quarks Q as having mass M that is larger than the mass m of the antiquarks \bar{q} . The ratio $f = m/M$ is a variable parameter.¹ The bound state problem in this model is solved by a numerical variational calculation; on the other hand it is analyzed in terms of an expansion in the size of the heavy bound QQ pair. We find that an analog of the parameter (116) in this solvable model is

$$\xi_c = N_c^6 f^4. \quad (117)$$

On the other hand we find from the numerical calculation that a stable tetron in this system exists only when the ratio f is smaller than a certain critical value $f_c(N_c)$,

$$f_c \approx a/N_c^{\frac{3}{2}} \quad (118)$$

where the coefficient a is of order one, numerically $a \approx 0.77$. It is thus plausible that the condition for

¹We consider, for simplicity, the situation where the heavier quarks are the same as well as the lighter antiquarks are the same. The consideration can be generalized to different masses in the limit of a strong mass hierarchy by introducing appropriate reduced masses.

existence of a stable tetron is a small value of the expansion parameter [in this model ξ_c in Eq. (117)] describing the deviation from the point-like model for the pair of heavy constituents.

Unlike in the solvable model with Coulomb-like forces, interactions in a system containing light u , d , or s quarks cannot be described by a potential. However some features of a gluon exchange can be applied to such systems in the limit of large number of colors N_c with the usual assumption [68] that, as N_c increases, the coupling α_s decreases, so that the product $N_c\alpha_s$ stays of order one. We discuss the parameters describing a tetron in this limit in Section 3.5.

3.4 A solvable model with superheavy quarks

We consider a system of two heavy quarks Q with mass M and two lighter (but still heavy) antiquarks \bar{q} with mass m each. For the start we assume no statistics symmetry constraints, e.g. assuming that the quarks are not identical, even though they have the same mass. The odd numbered positions \vec{r}_1 and \vec{r}_3 refer to quarks, while the even ones \vec{r}_2 and \vec{r}_4 are those for the antiquarks. The gluon exchange potential between the color constituents at positions \vec{r}_i and \vec{r}_j is

$$V_{ij} = T_{(i)}^a T_{(j)}^a d_{ij} \quad (119)$$

with $T_{(i)}^a$ being the color generators acting on the constituent at \vec{r}_i , and d_{ij} in the Coulomb limit is given by

$$d_{ij} = \frac{\alpha_s}{|\vec{r}_i - \vec{r}_j|} \quad (120)$$

The condition for the system to be colorless can be satisfied with two configurations of the sub-systems described by the color combinations:

$$\begin{aligned} \Psi &= (\bar{q}_{(2)\alpha} Q_{(1)}^\alpha)(\bar{q}_{(4)\beta} Q_{(3)}^\beta)/N_c \\ \Phi &= (\bar{q}_{(4)\alpha} Q_{(1)}^\alpha)(\bar{q}_{(2)\beta} Q_{(3)}^\beta)/N_c \end{aligned} \quad (121)$$

where α and β are color indices in the fundamental representation of the color group $SU(N_c)$. Clearly in the Ψ configuration the color singlets are $(\bar{q}_{(2)} Q_{(1)})$ and $(\bar{q}_{(4)} Q_{(3)})$ while in Φ they are $(\bar{q}_{(2)} Q_{(3)})$ and $(\bar{q}_{(4)} Q_{(1)})$.

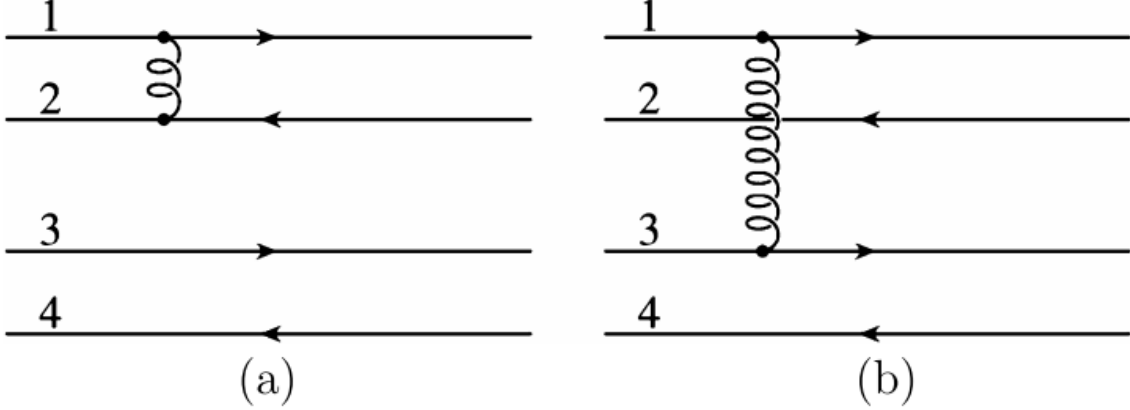


Figure 1: One-gluon exchanges in a tetron.

We derive the equation for the potential resulting from one-gluon exchanges among the constituents of a tetron.

Consider two types of gluon exchanges: between a quark and an antiquark, shown in Fig. 1 (a) and between a quark and another quark, Fig. 1 (b). The other four type are trivially related to these two.

In the Coulomb gauge, the dominant one-gluon scattering amplitude is

$$i\mathbb{M} = \left[\bar{\psi}_\alpha i g (t^a)_\beta^\alpha \gamma^0 \psi^\beta \right] \frac{i}{\bar{k}^2} \left[\bar{\psi}_\rho i g (t^a)_\sigma^\rho \gamma^0 \psi^\sigma \right], \quad (122)$$

where \bar{k} is the three-momentum carried by the gluon. We neglect the energy exchange since it is of a higher order of smallness in the case of Coulomb-like gluons [69]. The color coupling constant is g , $\alpha_s = \frac{g^2}{4\pi}$. Color matrices in the fundamental representation are denoted by t^a ; a useful identity is $\sum_a (t^a)_\beta^\alpha (t^a)_\sigma^\rho = \frac{1}{2}(\delta_\sigma^\alpha \delta_\beta^\rho - \frac{1}{N_c} \delta_\beta^\alpha \delta_\sigma^\rho)$ [70].

Consider now the gluon exchange in Fig. 1(a) when the initial state is

$$\begin{aligned} \psi &= \frac{1}{N_c} \left(\bar{q}_{(2)\alpha} Q_{(1)}^\alpha \right) \left(\bar{q}_{(4)\beta} Q_{(3)}^\beta \right) \\ &= \frac{1}{N_c} \delta_{\mu_1}^{\mu_2} \delta_{\mu_3}^{\mu_4} \left(\bar{q}_{(2)\mu_2} Q_{(1)}^{\mu_1} \right) \left(\bar{q}_{(4)\mu_4} Q_{(3)}^{\mu_3} \right). \end{aligned} \quad (123)$$

For the color indices in the final state we use indices ν_i with a subscript $i = 1 \dots 4$ describing the number of the constituent. Constituents 3 and 4 are spectators, not affected by this gluon exchange. We get the

following structure of the final state,

$$\begin{aligned}
i\mathbb{M}_{12} &\rightarrow i\frac{g^2}{k^2} \sum_a (t^a)_{\nu_1}^{\mu_1} (t^a)_{\nu_2}^{\nu_3} \delta_{\nu_3}^{\mu_3} \delta_{\mu_4}^{\nu_4} \frac{1}{N_c} \delta_{\mu_1}^{\mu_2} \delta_{\mu_3}^{\mu_4} \\
&= i\frac{g^2}{k^2} \frac{1}{2} (\delta_{\nu_2}^{\mu_1} \delta_{\nu_1}^{\nu_2} - \frac{1}{N_c} \delta_{\nu_1}^{\mu_1} \delta_{\mu_2}^{\nu_2}) \frac{1}{N_c} \delta_{\mu_1}^{\mu_2} \delta_{\nu_3}^{\nu_4} \quad (124)
\end{aligned}$$

$$= i\frac{g^2}{k^2} \frac{N_c^2 - 1}{2N_c} \frac{1}{N_c} \delta_{\nu_1}^{\nu_2} \delta_{\nu_3}^{\nu_4} \rightarrow i\frac{\alpha_s}{|\vec{r}_1 - \vec{r}_2|} \frac{N_c^2 - 1}{2N_c} \frac{1}{N_c} \delta_{\nu_1}^{\nu_2} \delta_{\nu_3}^{\nu_4} \quad (125)$$

where the last step transitions from momentum to configuration space. The color structure $\frac{1}{N_c} \delta_{\nu_1}^{\nu_2} \delta_{\nu_3}^{\nu_4}$ is again that of a Ψ state: since the $\{12\}$ pair is a color singlet in the initial state, a gluon exchange within that pair leaves it a singlet. The potential is obtained from the scattering amplitude by flipping its sign,

$$V_{12} = -\frac{N_c^2 - 1}{2N_c} \frac{\alpha_s}{|\vec{r}_1 - \vec{r}_2|}. \quad (126)$$

We recognize the attractive Coulomb potential with the coupling constant enhanced by the color factor $\frac{N_c^2 - 1}{2N_c}$ equal $\frac{4}{3}$ for $N_c = 3$. The result contributes $-\frac{N_c^2 - 1}{2N_c} d_{12}$ to the upper left term of the potential in eq. (129)

The exchange in Fig. 1(b), again with Ψ as the initial state, contributes to the potential

$$V_{13} = \frac{\alpha_s}{|\vec{r}_1 - \vec{r}_3|} \frac{1}{2} (\delta_{\nu_3}^{\mu_1} \delta_{\nu_1}^{\mu_3} - \frac{1}{N_c} \delta_{\nu_1}^{\mu_1} \delta_{\nu_3}^{\mu_3}) \delta_{\nu_2}^{\nu_4} \delta_{\mu_4}^{\nu_4} \frac{1}{N_c} \delta_{\mu_1}^{\mu_2} \delta_{\mu_3}^{\mu_4} \quad (127)$$

$$= \frac{\alpha_s}{|\vec{r}_1 - \vec{r}_3|} \frac{1}{2N_c} (\delta_{\nu_3}^{\nu_2} \delta_{\nu_1}^{\nu_4} - \frac{1}{N_c} \delta_{\nu_1}^{\nu_2} \delta_{\nu_3}^{\nu_4}). \quad (128)$$

Here we see both Ψ (the last term) and Φ (the first). This exchange contributes $-\frac{d_{13}}{2N_c}$ to the diagonal and $\frac{d_{13}}{2}$ to off-diagonal terms in the left column of the potential in eq. (129). In the same way we derive all the remaining d_{ij} terms in the potentials.

The sum of pairwise one-gluon exchanges among the four constituents results in the potential that can be written in terms of ψ and ϕ as

$$V \begin{pmatrix} \Psi \\ \Phi \end{pmatrix} = \frac{1}{2} \begin{pmatrix} -\frac{N_c^2 - 1}{N_c} (d_{12} + d_{34}) - \frac{1}{N_c} p & p \\ q & -\frac{N_c^2 - 1}{N_c} (d_{14} + d_{23}) - \frac{1}{N_c} q \end{pmatrix} \begin{pmatrix} \Psi \\ \Phi \end{pmatrix}, \quad (129)$$

where we have used the notation

$$p = d_{13} - d_{23} + d_{24} - d_{14}, q = d_{13} - d_{34} + d_{24} - d_{12}. \quad (130)$$

The potential matrix in Eq. (129) is not symmetric, because the color states Ψ and Φ in Eq. (121) are not orthogonal

$$\langle \Phi | \psi \rangle = \langle \psi | \phi \rangle = \frac{1}{N_c}. \quad (131)$$

Orthogonal (and normalized) states can be chosen as

$$u = \frac{1}{\sqrt{2(1+1/N_c)}}(\Psi + \Phi), \quad w = \frac{1}{\sqrt{2(1-1/N_c)}}(\Psi - \Phi), \quad (132)$$

and the one-gluon exchange potential (129) in the basis of these states reads as

$$V \begin{pmatrix} u \\ w \end{pmatrix} = -\frac{1}{4} \begin{pmatrix} \frac{N_c^2-1}{N_c}r - \frac{N_c-1}{N_c}(p+q) & \sqrt{N_c^2-1}s \\ \sqrt{N_c^2-1}s & \frac{N_c^2-1}{N_c}r + \frac{N_c+1}{N_c}(p+q) \end{pmatrix} \begin{pmatrix} u \\ w \end{pmatrix} \quad (133)$$

where

$$r = d_{12} + d_{34} + d_{14} + d_{23}, s = d_{12} + d_{34} - d_{14} - d_{23}. \quad (134)$$

The Hamiltonian with the potential (133) clearly has a $Z_2 \times Z_2$ symmetry under switching of the positions of the quarks, $\vec{r}_1 \leftrightarrow \vec{r}_3$, and (independently) switching the positions of the antiquarks, $\vec{r}_2 \leftrightarrow \vec{r}_4$. The symmetry of the u and w components is opposite; e.g. if the w component is even under swapping of quarks then the u component has to be odd. This implies that the eigenstates of the Hamiltonian can be classified in terms of the symmetry of the w component: w_{++}, w_{--}, w_{+-} and w_{-+} .

Furthermore, one can readily see that the states u and w contain the diquark (anti-diquark) pair of a definite color symmetry: symmetric in u and antisymmetric in w .² In particular, at $N_c = 3$ the u state contains a color sextet diquark (anti-sextet anti-diquark) pair, while the state w contains the anti-triplet diquark (triplet anti-diquark) pair configuration. Thus it is the latter w component that is present in the

²The color and coordinate symmetry properties of the components certainly become essential for identical quarks with the constraint of the Fermi–Dirac statistics. It should be noted however that even for identical quarks the constraints from the statistics can be satisfied by the appropriate spin state symmetry of the quarks. Thus, due to the suppression of spin-dependent interaction of heavy quarks, these constraints do not affect the conclusions about existence of stable bound systems in the limit of heavy quarks. Naturally the appropriate symmetry of the spin states constrains the overall quantum numbers, e.g. J^P of the tetron.

phenomenological analyses of Refs. [62], [63]. When the heavier quarks Q are close to each other, the term d_{13} becomes dominant, $(p + q) \approx 2d_{13}$, and one recovers from eq. (133) the attraction in the color antisymmetric state,³

$$V_{13} = -\frac{N_c + 1}{2N_c} d_{13}. \quad (135)$$

This attraction binds the Q quarks into a compact Coulomb-like system with the size and energy becoming, at large N_c ,

$$r_{QQ} \sim (M\alpha_s)^{-1}, E_{QQ} \sim M\alpha_s^2 \quad (136)$$

Clearly, at large M such distance scale is small in the scale R_q of the dynamics of the lighter antiquarks in the considered system, and one can consider an expansion in the ratio r_{QQ}/R_q . In the zeroth order of this expansion, i.e. at vanishing r_{QQ} , the off-diagonal terms in eq. (133) vanish and there is no mixing between the w and u components, and thus one can set $u = 0$. Then the leading at large N_c interaction for the lighter antiquarks is that with the heavier quarks. After setting $\vec{r}_3 = \vec{r}_1$ in the proportional to N_c part of the diagonal term in eq. (133) one finds the potential

$$V_{qQ} = -\frac{N_c}{2}(d_{12} + d_{14}), \quad (137)$$

describing an independent Coulomb-like interaction of the two lighter antiquarks with the compact QQ system. Naturally, the latter interaction corresponds to spectra of two independent $Q\bar{q}$ Coulomb-like quarkonia, with the distance and energy scale set as

$$R_q \sim (mN_c\alpha_s)^{-1}, \quad E_q \sim mN_c^2\alpha_s^2. \quad (138)$$

It is also clear that the ground state in both the potential (135) and (137) is spatially symmetric, so that the overall ground state of the tetron is of the type w_{++} under the $Z_2 \times Z_2$ symmetry.

Due to the binding between the heavy quarks by the potential (135) the resulting four-quark system is stable under decay to two quarkonium mesons. It should be noted however that this binding is only sub leading in terms of the large N_c counting, as can be seen by comparing the expressions (135) and (137).

Thus the discussed ‘hierarchy’ of the binding energies is only applicable if the ratio f of the masses is small

³It can be also mentioned that in the same limit of closely separated heavier quarks their interaction in the color symmetric state (the u component) is a repulsion: $V_{13} = (N_c - 1)d_{13}/2N_c$.

enough at a fixed N_c . In other words there is a critical value of this ratio $f_c(N_c)$ above which the described approximation fails. In order to evaluate the behavior of $f_c(N_c)$ we consider here the effects arising at a finite ratio r_{QQ}/R_q . We find that the main effect arises due to non-vanishing off-diagonal elements in the potential (133):

$$\sqrt{N_c^2 - 1}(d_{12} + d_{34} - d_{14} - d_{23}) \sim N_c \alpha_s r_{QQ} / R_q^2. \quad (139)$$

This term can be considered as small as long as the energy shift that it produces in the second order is small in comparison with either of the energy scales [in eq. (136) or 138]. One can readily verify that using the energy scale imposes a more stringent bound on $f = m/M$:

$$(N_c \alpha_s r_{QQ} / R_q^2)^2 / E_{QQ}^2 \sim N_c^6 (m/M)^4 \ll 1 \quad (140)$$

so that the applicability of the discussed expansion fails at $f > f_c(N_c)$ with f_c given by eq. (118). In particular the absence of a stable bound state at larger mass ratio makes highly unlikely existence of a “double bottomonium” occasionally discussed in the literature (see e.g. Ref. [71], [72], [62]).

By performing a numerical variational calculation we find that the lowest bound state in the system is of the w_{++} type and exists only when the ratio in eq. (140) is small so that the mass ratio f is smaller than the critical value described by eq. (118) (see Fig. 2).⁴ The results for the values of f_c at which the bound state disappears at different N_C are shown in Fig. 3.

We computed the data points in Fig. 3 with a generalization of the algorithm developed for the positronium molecule [14]. We use the potential V in Eq. (133) in a non-relativistic Schrödinger equation. We work in the rest frame of the tetron. Both wave-function components u and w are represented as a sum of Gaussian trial functions of all six inter-particle distances, for example

$$\psi_u = \sum_{k=1}^{N_B} c_k \exp(-\sum_{i,j} a_{ijk} r_{ij}^2), \quad (141)$$

where r_{ij} are the pair-wise distances between the constituents, and N_B is the size of the basis of trial functions. We use $N_B = 200$ for each of the two components. (Much larger bases can be employed if higher precision is warranted.) Thus there are $2 \times 6N_B = 2400$ variational parameters a_{ijk} . We adjust

⁴We note in passing that a shallower bound state of the type w_{--} also exists at sufficiently small f , while no bound states of mixed symmetry w_{+-} or w_{-+} are found in our analysis.

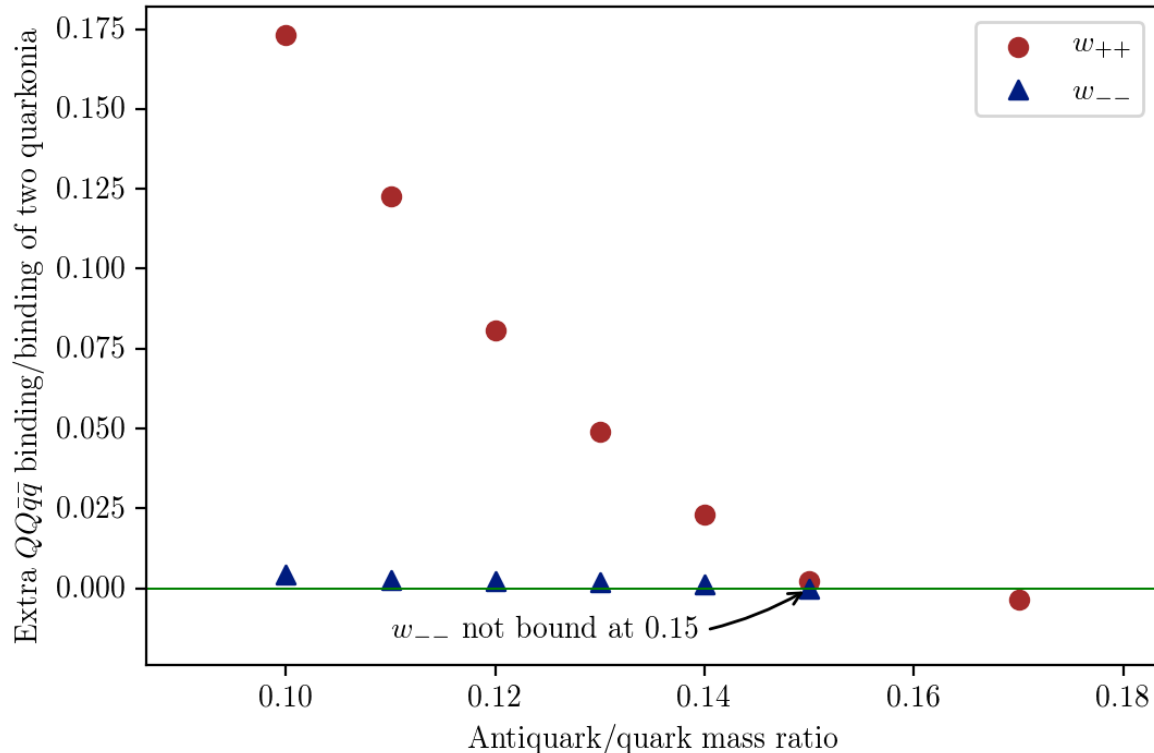


Figure 2: Extra binding energy of a tetron (in units of the total binding of two independent $Q\bar{q}$ mesons) as a function of the antiquark/quark mass ratio f . The state with the symmetry w_{++} (circles) is bound strongly than w_{--} (triangles). Even the state w_{++} is no longer bound when the mass ratio exceeds about $f_c \approx 0.152$. The number of colors is $N_c = 3$.

them to find a configuration minimizing the ground-state energy.

A challenge in this calculation is a slow convergence very near the threshold. This may explain the slight spread of the data points around the fitted curve in Fig. 2.

3.5 Tetron with superheavy quarks and massless antiquarks

A potential description, and even more in terms of a Coulomb-like potential, is not applicable for the interaction of light u, d, s quarks, and other methods have to be invoked. In this section we consider a system of two very heavy quarks QQ with mass M each, and two massless anti-quarks $\bar{q}\bar{q}$ (which are not necessarily identical, e.g. $\bar{u}\bar{d}$). Although literally the potential model of the previous section does not apply, some essential features of the interaction in eq. (133) are retained, in particular a Coulomb-like

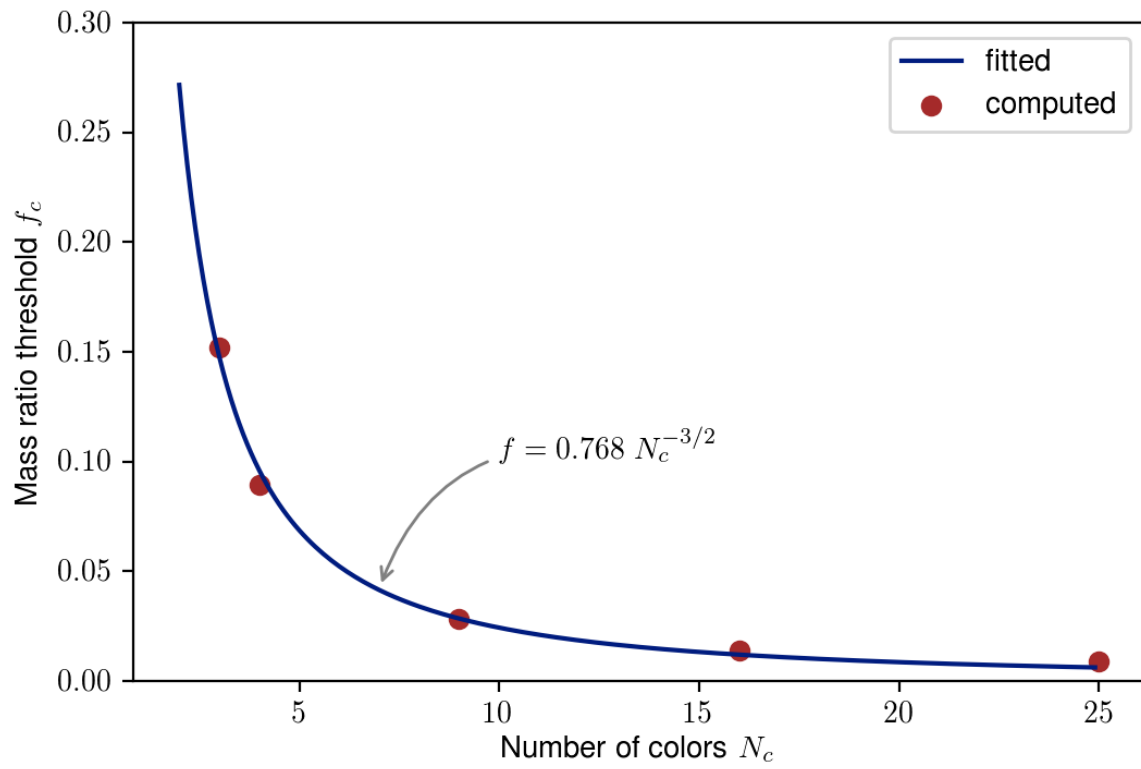


Figure 3: Mass threshold f_c for tetrons as a function of the number of colors. The curve is the fit of the numerically computed values of f_c to the formula in eq. (118).

potential treatment of the interaction between the heavy quarks. Namely, the one gluon exchange between the heavy quarks still produces a compact bound state in the potential (135) with the relevant parameters described by eq. (136). This interaction, essential at large M , is however only sub-dominant in the large N_c limit, in which limit the dominant effect (of order one) is the interaction between the light and heavy constituents. The heavy-light mesons $Q\bar{q}$ are formed and the estimate (138) for the relevant characteristic size and energy scale is replaced by

$$R_q \sim \Lambda_{QCD}^{-1}, E_q \sim \Lambda_{QCD}. \quad (142)$$

Moreover, the mixing between the w and u components, although not describable by a potential analog of the non-diagonal components in eq. (133), retains the following features. It is of order one in the limit of large N_c and it vanishes at zero spatial separation r_{QQ} between the heavy quarks. Thus one can estimate the amplitude of the mixing in the linear order of the expansion in r_{QQ} as

$$\langle u|H|w \rangle \sim r_{QQ}/R_q^2 \sim r_{QQ}\Lambda_{QCD}^2 \quad (143)$$

The perturbation parameter for the mixing is then evaluated as

$$\xi \sim \frac{|\langle u|H|w \rangle|^2}{E_{QQ}^2} \sim \frac{\Lambda_{QCD}^4}{M^4\alpha_s^6} \quad (144)$$

which results in the estimate in eq. (116)

Chapter 4

Conclusion

In the first part of the work presented here, we used the variational method in Gaussian basis and combined it with the algorithms for decomposing the Hamiltonian matrix elements and for optimizing the wave function for PsH. Using these optimized wave functions with 1000 basis, we calculated the various properties, such as inter-particle distances and the non-relativistic ground state energy and compare these quantities with the one calculated in [2]. Our result for the binding energy is comparable to the one calculated in [2, 55].

In the second part of the work, we discussed the stability of mesonic four quark system $Q_a Q_b \bar{q} \bar{q}$, where Q and q denote the heavy and light quarks respectively. We found that the parameter ξ in eq. (116), similarly to ξ_c in (117), controls the applicability of the treatment of tetron starting from a compact bound diquark made of the heavy quarks. A perturbative expansion in the spatial separation is possible when this parameter is (formally) much less than one, and generally this expansion becomes invalid once the ξ is of order one. Our calculations in the solvable model with heavy quarks however revealed not only that the expansion becomes inapplicable when ξ_c is of order one, but no stable bound tetrans arise at all. We interpret this behavior as that the leading at large N_c dipole force [the off-diagonal terms in the potential (133)] results in a strong mixing between the w and u components. Such mixing essentially randomizes the total color of heavy diquark, so that a residual net interaction between the heavy constituents largely cancels between the color symmetric and antisymmetric configurations. We thus conclude that it is highly likely that in a more realistic tetron with light quarks the existence of a stable bound state is also controlled by the parameter ξ , and the stability does not exist if ξ is of order one or larger.

It is certainly of a primary interest to understand the status of tetrans with the heavy constituents being the actual b and c quarks. Using the criterion based on the estimate in eq. (116) one readily concludes that for the $cc\bar{q}\bar{q}$ and $bc\bar{q}\bar{q}$ systems, where the reduced mass M in the heavy diquark is determined by the charm quark mass, there is essentially no chance that the parameter ξ is small. Thus we confirm the finding of the earlier studies [12] that it is highly unlikely that there are stable tetrans with such quark structure.

The parameter ξ from eq. (116) is more likely to be small enough, if M is proportional to the mass of

the b quark. Due to the inherent uncertainty in this estimate for a nonperturbative system it would be impossible to unambiguously claim existence of stable tetrons of such type, based solely on this estimate. However we believe that there is a strong indication that if stable tetrons do exist, the only possibility for them is to be of the double bottom type. At this point we find an agreement with the conclusions based on purely phenomenological estimates in Refs. [62, 63]. It is certainly understood [63] that an experimental observation of double bottom tetrons can be quite challenging. However a search for them may be well worth the effort, as the tetrons possibly present a very unconventional form of hadrons that are stable with respect to strong decay.

Clearly, the smallness of the parameter ξ , or its analog, requires existence of two strongly separated mass scales, whose ratio can ensure that the binding effect in the color antisymmetric state due to heavy masses is not eliminated by a larger in N_c destabilizing mixing between the color states. We notice absence of such hierarchy of scales for four-quark systems with only the heavy b and c quarks, e.g. $b\bar{b}\bar{c}$, so that we do not expect existence of stable tetrons of such type. The same negative conclusion applies to four-quark systems with hidden heavy flavors, such as a double bottomonium $b\bar{b}\bar{b}$, or double charmonium, $c\bar{c}\bar{c}$ systems.

References

- [1] A. Czarnecki, B. Leng, and M. Voloshin, *Stability of Tetrons*, Physics Letters B **778**, 233–238 (2018).
- [2] J. Mitroy, *Energy and Expectation Values of the PsH System*, Physical Review A **73**, 054502 (2006).
- [3] W. H. Press, S. A. Teukolsky, W. T. Vetterling, and B. P. Flannery, *Numerical Recipes: The Art of Scientific Computing*, Cambridge University Press, Cambridge, UK, 3rd edition (2007).
- [4] S. Mohorovicic, *Moeglichkeit Neuer Elemente Und Ihre Bedeutung für Die Astrophysik*, Astronomische Nachrichten **253**, 93 (1934).
- [5] M. Deutsch and E. Dulit, *Short Range Interaction of Electrons and Fine Structure of Positronium*, Physical Review **84**, 601 (1951).
- [6] A. Ali, J. S. Lange, and S. Stone, *Exotics: Heavy Pentaquarks and Tetraquarks*, Progress in Particle and Nuclear Physics **97**, 123–198 (2017).
- [7] F.-K. Guo, C. Hanhart, U.-G. Meißner, Q. Wang, Q. Zhao, and B.-S. Zou, *Hadronic Molecules*, Reviews of Modern Physics **90**, 015004 (2018).
- [8] M. B. Voloshin and L. B. Okun, *Hadron Molecules and Charmonium Atom*, Pisma Zh. Eksp. Teor. Fiz **23** (1976), JETP Lett. 23, 333.
- [9] A. Esposito, A. Pilloni, and A. D. Polosa, *Multiquark Resonances*, Phys. Rep. **668**, 1 (2017).
- [10] S. Dubynskiy and M. B. Voloshin, *Hadro-charmonium*, Physics Letters B **666**, 344–346 (2008).
- [11] H. J. Lipkin, *A Model-independent Approach to Multiquark Bound States*, Physics Letters B **172**, 242–247 (1986).
- [12] J.-P. Ader, J.-M. Richard, and P. Taxil, *Do Narrow Heavy Multiquark States Exist?*, Physical Review D **25**, 2370 (1982).
- [13] B. Galerkin, *On Electrical Circuits for the Approximate Solution of the Laplace Equation*, Vestnik Inzh. **19**, 897–908 (1915).

- [14] M. Puchalski and A. Czarnecki, *Dipole Excitation of the Positronium Molecule Ps_2* , Physical Review Letters **101**, 183001 (2008).
- [15] J. MacDonald, *Successive Approximations by the Rayleigh-Ritz Variation Method*, Physical Review **43**, 830 (1933).
- [16] K. Pachucki and J. Komasa, *Gaussian Basis Sets with the Cusp Condition*, Chemical Physics Letters **389**, 209–211 (2004).
- [17] P. A. M. Dirac, *The Quantum Theory of the Electron*, Proceedings of the Royal Society of London. Series A **117**, 610–624 (1928).
- [18] C. D. Anderson, *The Positive Electron*, Phys. Rev. **43**, 491–494 (1933).
- [19] J. A. Wheeler, *Polyelectrons*, Annals of the New York Academy of Sciences **48**, 219–238 (1946).
- [20] A. Ore, *The Existence of Wheeler-Compounds*, Physical Review **83**, 665 (1951).
- [21] E. A. Hylleraas, *Neue Berechnung der Energie des Heliums im Grundzustande, sowie des Tiefsten Terms von Ortho-Helium*, Zeitschrift für Physik **54**, 347–366 (1929).
- [22] K. Strasburger and H. Chojnacki, *On the Reliability of the SCF and CI Wavefunctions for Systems Containing Positrons*, Chemical Physics Letters **241**, 485–489 (1995).
- [23] S. L. Saito, *Calculation of Positronium Compounds, $PsLi$, PsF , and $PsCl$, by Second-order Variational Perturbation Method*, Chemical Physics Letters **245**, 54–58 (1995).
- [24] V. Gol'danskii, A. Ivanova, and E. Prokop'ev, *Annihilation of Positrons in Alkali Metal Hydrides*, Soviet Physics JEPT **20** (1965).
- [25] O. G. Ludwig and R. G. Parr, *Configuration Interaction Wavefunction for Positronium Hydride*, Theoretica Chimica Acta **5**, 440–445 (1966).
- [26] S. L. Saito, *Multireference Configuration Interaction Calculations of Some Low-lying States of Positronium Hydride*, The Journal of Chemical Physics **118**, 1714–1720 (2003).
- [27] M. Bromley and J. Mitroy, *Configuration-interaction Calculations of PsH and e^+Be* , Physical Review A **65**, 012505 (2001).

- [28] D. C. Clary, *Configuration-interaction-Hylleraas Calculations on One-positron Atomic Systems*, Journal of Physics B: Atomic and Molecular Physics **9**, 3115 (1976).
- [29] S. Bubin and L. Adamowicz, *Nonrelativistic Variational Calculations of the Positronium Molecule and the Positronium Hydride*, Physical Review A **74**, 052502 (2006).
- [30] G. Ryzhikh and J. Mitroy, *Positron Annihilation Profiles for HPs and $He(3S^e)e^+$* , Journal of Physics B: Atomic, Molecular and Optical Physics **32**, 4051 (1999).
- [31] K. Strasburger and H. Chojnacki, *Quantum Chemical Study of Simple Positronic Systems Using Explicitly Correlated Gaussian Functions— PsH and $PsLi^+$* , The Journal of Chemical Physics **108**, 3218–3221 (1998).
- [32] J. Usukura, K. Varga, and Y. Suzuki, *Signature of the Existence of the Positronium Molecule*, Physical Review A **58**, 1918 (1998).
- [33] A. M. Frolov and V. H. Smith, *Ground State of Positronium Hydride*, Physical Review A **56**, 2417 (1997).
- [34] A. M. Frolov and V. H. Smith, *Positronium Hydrides and the Ps_2 Molecule: Bound-state Properties, Positron Annihilation Rates, and Hyperfine Structure*, Physical Review A **55**, 2662 (1997).
- [35] A. M. Frolov, *Semi-exponential Basis for Highly Accurate Computations of Three-electron Atomic Systems*, Physics Letters A **374**, 2361–2366 (2010).
- [36] D. Woods, *Variational Calculations of Positronium Scattering with Hydrogen*, Arxiv Preprint Arxiv:1508.05681 (2015).
- [37] P. Van Reeth and J. Humberston, *Low Energy Positronium–hydrogen Scattering*, Nuclear Instruments and Methods in Physics Research Section B: Beam Interactions with Materials and Atoms **221**, 140–143 (2004).
- [38] Z.-C. Yan and Y. Ho, *Ground State and S-wave Autodissociating Resonant States of Positronium Hydride*, Physical Review A **59**, 2697 (1999).
- [39] Y. Ho, *A Resonant State and the Ground State of Positronium Hydride*, Physical Review A **17**, 1675 (1978).

- [40] Y. Ho, *Positron Annihilation in Positronium Hydrides*, Physical Review A **34**, 609 (1986).
- [41] S. Neamtan, G. Darewych, and G. Oczkowski, *Annihilation of Positrons from the H^-e^+ Ground State*, Physical Review **126**, 193 (1962).
- [42] C. F. Lebeda and D. M. Schrader, *Towards an Accurate Wave Function for Positronium Hydride*, Physical Review **178**, 24 (1969).
- [43] P. Nevin, D. Schrader, and C. Lebeda, *An Improved Wave Function for Positronium Hydride: Preliminary Report*, Applied Physics **3**, 159–160 (1974).
- [44] S. Houston and R. J. Drachman, *Comment on the Ground State of Positronium Hydride*, Physical Review A **7**, 819 (1973).
- [45] B. Page and P. Fraser, *The Ground State of Positronium Hydride*, Journal of Physics B: Atomic and Molecular Physics **7**, L389 (1974).
- [46] S. Chiesa, M. Mella, and G. Morosi, *Quantum Monte Carlo Estimators for the Positron-Electron Annihilation Rate in Bound and Low-Energy Scattering States*, Physical Review A **69**, 022701 (2004).
- [47] D. Bressanini, M. Mella, and G. Morosi, *Stability and Positron Annihilation of Positronium Hydride $L=0, 1, 2$ States: A Quantum Monte Carlo Study*, Physical Review A **57**, 1678 (1998).
- [48] N. Jiang and D. Schrader, *Diffusion Quantum Monte Carlo Calculation of the Binding Energy and Annihilation Rate of Positronium Hydride, PsH*, The Journal of Chemical Physics **109**, 9430–9433 (1998).
- [49] M. Mella, G. Morosi, and D. Bressanini, *Positron and Positronium Chemistry by Quantum Monte Carlo. IV. Can This Method Accurately Compute Observables beyond Energy?*, The Journal of Chemical Physics **111**, 108–114 (1999).
- [50] T. Yoshida and G. Miyako, *Diffusion Quantum Monte Carlo Calculations of Positronium Hydride and Positron Lithium*, Physical Review A **54**, 4571 (1996).
- [51] J. Rychlewski, *Explicitly Correlated Wave Functions in Chemistry and Physics: Theory and Applications*, volume 13, Springer Science & Business Media (2013).

- [52] D. Bressanini and G. Morosi, *Compact Boundary-Condition-Determined Wave Function for Positronium Hydride (PsH)*, The Journal of Chemical Physics **119**, 7037–7042 (2003).
- [53] C. Le Sech and B. Silvi, *Study of Positronium Hydride with a Simple Wavefunction: Application to the Stark Effect of Psh*, Chemical Physics **236**, 77–85 (1998).
- [54] Z.-C. Yan and Y. Ho, *Relativistic Effects in Positronium Hydride*, Physical Review A **60**, 5098 (1999).
- [55] S. Bubin and K. Varga, *Ground-state Energy and Relativistic Corrections for Positronium Hydride*, Physical Review A **84**, 012509 (2011).
- [56] R. J. Drachman, *The Interaction of Positrons and Positronium with Small Atoms*, Canadian Journal of Physics **60**, 494–502 (1982).
- [57] D. Schrader, F. M. Jacobsen, N.-P. Frandsen, and U. Mikkelsen, *Formation of Positronium Hydride*, Physical Review Letters **69**, 57 (1992).
- [58] G. Ryzhikh, J. Mitroy, and K. Varga, *The Structure of Exotic Atoms Containing Positrons and Positronium*, Journal of Physics B: Atomic, Molecular and Optical Physics **31**, 3965 (1998).
- [59] H. Chen, S. C. Wilks, J. D. Bonlie, E. P. Liang, J. Myatt, D. F. Price, D. D. Meyerhofer, and P. Beiersdorfer, *Relativistic Positron Creation Using Ultraintense Short Pulse Lasers*, Physical Review Letters **102**, 105001 (2009).
- [60] P. McGrath, *On the Application of Effective Field Theory Methods to Polyelectrons* (2010).
- [61] R. Aaij et al., *Observation of the Doubly Charmed Baryon Ξ_{cc}^{++}* , Phys. Rev. Lett. **119**, 112001 (2017), 1707.01621.
- [62] M. Karliner and J. L. Rosner, *Discovery of Doubly-charmed Ξ_{cc} Baryon Implies a Stable $(bb\bar{u}\bar{d})$ Tetraquark*, Phys. Rev. Lett. **119**, 202001 (2017), 1707.07666.
- [63] E. J. Eichten and C. Quigg, *Heavy-quark Symmetry Implies Stable Heavy Tetraquark Mesons $Q_i Q_j q_k q_l$* , Physical Review Letters **119**, 202002 (2017).
- [64] A. Francis, R. J. Hudspith, R. Lewis, and K. Maltman, *Lattice Prediction for Deeply Bound Doubly Heavy Tetraquarks*, Phys. Rev. Lett. **118**, 142001 (2017), 1607.05214.

- [65] P. Bicudo, J. Scheunert, and M. Wagner, *Including Heavy Spin Effects in the Prediction of a $\bar{b}bud$ Tetraquark with Lattice QCD Potentials*, Phys. Rev. **D95**, 034502 (2017), 1612.02758.
- [66] S. Zouzou, B. Silvestre-Brac, C. Gignoux, and J. M. Richard, *Four Quark Bound States*, Z. Phys. **C30**, 457 (1986).
- [67] J. Vijande, A. Valcarce, and N. Barnea, *Exotic Meson-meson Molecules and Compact Four-quark States*, Phys. Rev. **D79**, 074010 (2009), 0903.2949.
- [68] G. 't Hooft, *A Planar Diagram Theory for Strong Interactions*, Nucl. Phys. **B72**, 461 (1974), [,337(1973)].
- [69] A. Pineda, *Review of Heavy Quarkonium at Weak Coupling*, Progress in Particle and Nuclear Physics **67**, 735–785 (2012).
- [70] Muta, Taizo, *Foundations of Quantum Chromodynamics: an Introduction to Perturbative Methods in Gauge Theories*, volume 5, World Scientific Publishing Company, Singapore (1987).
- [71] A. V. Berezhnoy, A. V. Luchinsky, and A. A. Novoselov, *Tetraquarks Composed of 4 Heavy Quarks*, Phys. Rev. **D86**, 034004 (2012), 1111.1867.
- [72] N. Brambilla, G. Krein, J. Tarrús Castellà, and A. Vairo, *Long-range Properties of $1s$ Bottomonium States*, Phys. Rev. **D93**, 054002 (2016), 1510.05895.
- [73] M. J. Hopper, *Harwell Subroutine Library: A Catalogue of Subroutines*, Atomic Energy Research Establishment, London (1984).

Appendix A: Documentation of the Variational Method coded in Fortran

We apply the variational method to numerically solve the non-relativistic Schrödinger equation for a few-body system. One can define the properties of a system of particles such as the mass and charge of each particle and our program (we call it VM) finds the ground state energy and its corresponding wave function. The VM uses the inverse iteration method to solve the generalized eigenvalue problem and it only returns the lowest eigenstate. Our optimization algorithm searches iteratively the best parameters for an ansatz. The program will terminate when the result reaches a desired accuracy specified by the user. The wave function contains essentially all the information about the system. We can extract the property of system by calculating the expectation value of the corresponding operator from the wave function.

Figure (4) shows the directories and files contained in VM.

The main file of VM is the *VM.f* file. It utilizes four modules which are “*Tables*”, “*PRMITS*”, “*bodysym*” and “*optimize*”. The “*Tables*”, “*PRMITS*” modules are all located in the file *mystd/prmts.f* and they contain all the global variables used throughout the program. The module “*bodysym*” contains the definition of the physical system of interest. A definition of a new particle system must use this name. The module “*Optimize*” locates in *VA04AD.f* file. This module contains two subroutines: “*loopsearch*”, which manages the Powell method optimization scheme (PMOS), and “*VA04AD*”, which is an algorithm for non-derivative minimization and is taken from the Harwell Subroutine Library [73]. In each iteration of PMOS, VA04AD is used to tune the variables of a single basis function while keeping others constant. PMOS also utilizes the *QR update* procedure to speed up the program.

A standard workflow of the VM program is as follows:

1. Defining the physical system;
2. Solving the system to obtain the wave function; and
3. Repetitively optimizing the ansatz until the precision criteria are reached.

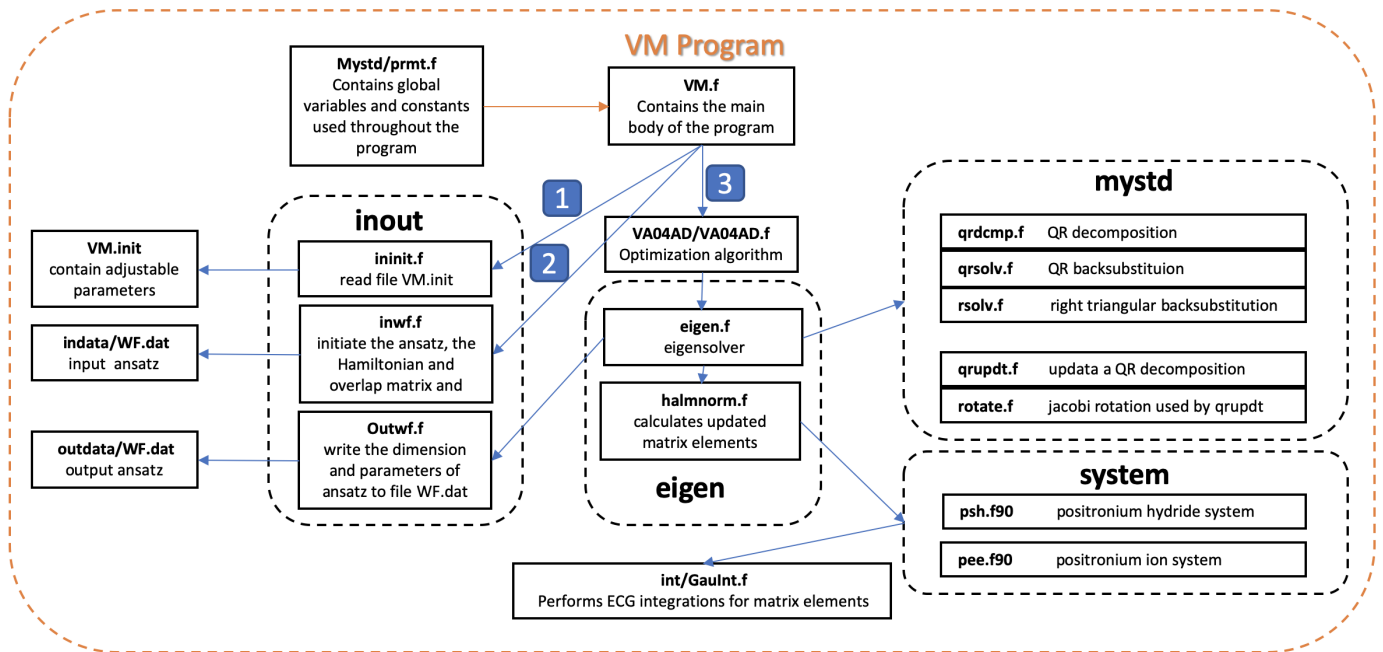


Figure 4: Directories and files contained in VM. The boxes with dash line represent a folder and every rigid box is a Fortran file. The blue arrows point to the files which are called by the given file. The blue boxes are used to order the process of the main program. `Mystd/prmt.f` contains global variables and constants used throughout the program, thus a red arrow is used. The 5 files in the `mystd` directory are taken from ref. [3].

Defining the physical system

A quantum few-body system is specified via a module locating at the “*/VM/system*” folder. Each module contains recipes for calculating the matrix elements. In order to construct the Hamiltonian matrix correctly, users provide the essential information of a system such as the number of particles, the mass and charge of each particle, and an initial guess of the energy of the system. Users also specify the symmetrization rules in order to calculate the matrix element successfully. The function “*matrele*” calculates the Hamiltonian matrix elements (hm) and overlap matrix element (om, calculated by “*overlap*” function). The Hamiltonian matrix elements consist of the kinetic energy (calculated by “*kin_part*” function) and the potential energy (calculated by “*pfv*” function) terms.

Solving the system

We select the correct module to compile. This can be done by switching the argument of the variable *system= [name of the file without extension]* in the file *VM/makefile*. We run the program through a command *\$ make* , then *\$./main*. Every time the PMOS finds a lower energy state, the magnitude and error of this energy is displayed. VM stores the wave function parameters in *outdata/WF.dat* file.

The implemented eigensolver affects VM’s accuracy and speed. In the following chapter, we discuss the algorithms used in our eigensolver.

Eigensolver

VM constructs the general eigenvalue problem by using the “hamlnorm” subroutine. This file calculates matrix elements according to the supplied recipes and parameter from the ansatz. There are two situations. In the first case, we calculate every matrix element and this case happens in the beginning when the Hamiltonian and overlap matrix are blank. Then VM calls the “eigen” subroutine to solve for the lowest eigenstate and eigenvector. Specifically, it uses the inverse iteration method together with the QR decomposition and the back substitution method to solve the general eigenvalue program.

In the second case, VM only calculates the arrays of matrix elements affected by the updated parameters. At this time, VM calls the QR update recipe instead of performing a new QR decomposition. Whenever the “eigen” function finds a lower energy state, it automatically writes all parameters of the ansatz to the

output file “outdata/WF.dat”.

Inverse iteration

To solve the generalized eigenvalue problem eq. (19), we employ the inverse iteration method [3]. This procedure only determines one eigenenergy and its corresponding eigenvector. In the n^{th} iteration, we have a trial eigenvector, $|\psi_n\rangle$ and an estimation of the eigenenergy E_n . The next step is to solve $|\chi_n\rangle$ from the following linear system,

$$(H - E_n S) |\chi_n\rangle = S |\psi_n\rangle \quad (145)$$

It can be shown that the new eigenvector $|\chi_n\rangle$ will be closer to the true eigenvector corresponding to the true energy E than $|\psi_n\rangle$ by a factor of $(E - E_n)^{-1}$ [3]. In the next iteration, we use the normalized vector

$$|\psi_{n+1}\rangle = \frac{|\chi_n\rangle}{\sqrt{\langle \chi_n | \chi_n \rangle}} \quad (146)$$

as our new trial vector. We update our estimate of the eigenenergy to

$$E_{n+1} = E_n + \frac{\langle \chi_n | S | \psi_n \rangle}{\langle \chi_0 | S | \chi_0 \rangle}. \quad (147)$$

The eigenvector converges rapidly after several iterations. Since we are only interested in the ground state, we have the advantage of keeping the initially guessed eigenenergy E_n consistent throughout the calculation. The initial value of E_n should be a lower bound estimation of the system’s energy level.

QR Decomposition

We solve the linear system eq. (145) by using the QR decomposition and the back substitution method. The goal of QR decomposition is to decompose a matrix into a product of an orthogonal matrix Q and an upper triangular matrix R

$$(H - E_n S) = QR, \quad (148)$$

where Q has the property

$$Q^T Q = I. \quad (149)$$

We use the Numerical Recipe routine *NR::qrdcmp* to complete this step [3]. The Numerical Recipe routine utilizes Householder transformation. The linear system eq. (145) is rewritten as

$$R |\chi_n\rangle = Q^T S |\psi_n\rangle. \quad (150)$$

The back substitution method solves a linear system $Ax = b$ where A is an upper triangular $N \times N$ matrix. It begins with the last row, where the value of $|\chi_n\rangle [N]$ is given. Then it moves to the second last equation and back-substitutes the value of the previously calculated off-diagonal terms to calculate the $|\chi_n\rangle [N - 1]$. It repeats the process until all the components of $|\chi_n\rangle$ have been obtained. When we keep E_n to be a constant, it keeps the matrix $(H - E_n S)$ to be the same so that the matrix QR is also the same in every inverse iteration.

QR update

We only alternate one basis function at a time in the PMOS. The other basis functions are kept constant if they have not been selected for this round. If we alter the parameter of the k^{th} base function, it will affect the k^{th} row and the column of the Hamiltonian and overlap matrix. Our goal is to find a new QR decomposition for the perturbed linear system eq. (145)

$$(H' - E_n S') |\chi_n\rangle = S |\psi_n\rangle. \quad (151)$$

It turns out there is method called *QR update*, which relates QR matrix of the perturbed matrix to the old one. The QR decomposition is an $O(N^3)$ algorithm, and the QR update is an $O(N^2)$ algorithm [3]. There exists a speed advantage at higher dimensions. The QR update has the advantage of choosing the QR decomposition method for solving the generalized eigenvalue problem coupling with the PMOS.

The QR update works if the change of the linear system eq. (145) is in the form,

$$A' \rightarrow A + \vec{S} \otimes \vec{T}; \quad (152)$$

\vec{S} and \vec{T} are vectors, a matrix $W = \vec{S} \otimes \vec{T}$ denotes the outer product of \vec{S} and \vec{T} , such that $W_{ij} = \vec{S}_i \vec{T}_j$.

In our case, the change is

$$(H' - E_n S') = (H - E_n S) + \vec{V} \otimes \vec{e}_k + \vec{e}_k \otimes \vec{V}, \quad (153)$$

\vec{e}_k is the Cartesian basis vector. The updated vector \vec{V} is constructed from the influenced arrays of the Hamiltonian matrix and overlap matrix as following

$$\vec{V}_i = \begin{cases} (H'_{ik} - E_n S'_{ik}) - (H_{ik} - E_n S_{ik}) & i \neq k \\ \frac{1}{2}[(H'_{ik} - E_n S'_{ik}) - (H_{ik} - E_n S_{ik})] & i = k \end{cases}. \quad (154)$$

We apply the QR update method twice to find new Q' and R' matrices for $Q'R' = H' - E_n S'$. Luckily, the QR update is also a standard routine[3].

Optimization

Powell method Optimization Scheme (PMOS)

We implemented an efficient serial optimization scheme as shown in Fig. (5). In the initialization stage, VM prepares the initial trial wave function and constructs the Hamiltonian matrix and the Overlap matrix eq. (13, 14). It also computes the corresponding eigenvalue. Then, VM enters a “while loop” and it stops when the accuracy of the variational energy reach the desired criteria. During each iteration, VM employs the Powell method to find the optimal parameters which give the lowest variational energy. The Powell method fine tunes the parameters of only one basis function at a time while keeping other parameters constant. Every time VM finds a lower energy, it synchronizes the table recording the parameters of the wave function with the trial function giving the lowest energy found so far.

Powell Method

We minimize the eigenenergy which is a function of the parameters in a single basis function. Calculation of the gradient of the eigenenergy is not practical. We choose the Powell method to solve this optimization problem. This multidimensional and non-derivative minimization method consists of sequences of line minimizations. The definition of this sub-algorithm is given in Numerical Recipes [3]: “Given as input the

Powell method optimization scheme (PMOS)

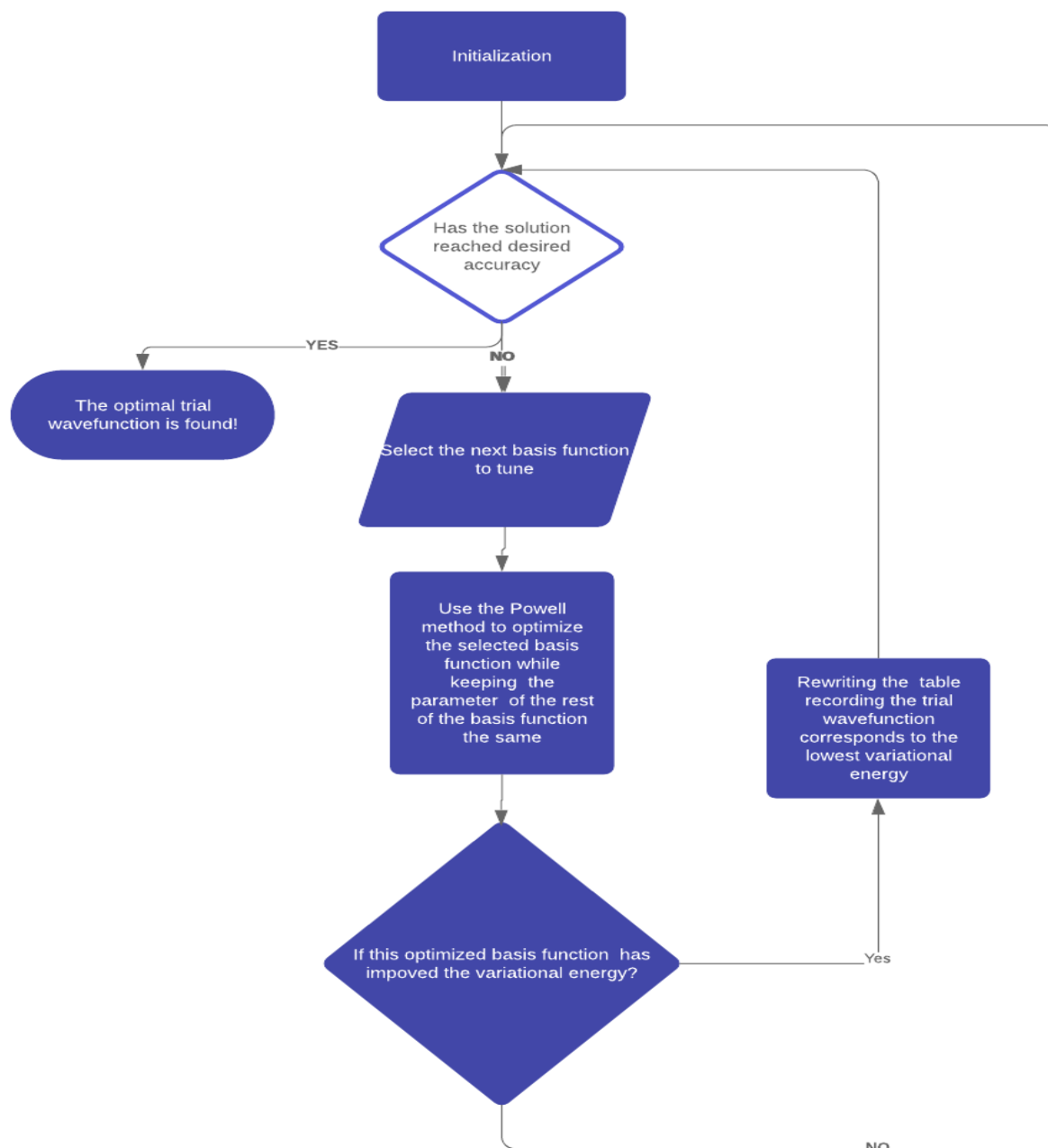


Figure 5: Powell Method Optimization Scheme (PMOS).

vectors P and n , and the function f of one variable, find the scalar λ that minimizes $f(P + \lambda n)$, replace P by $P + \lambda n$ and then replace n by λn ." Successive minimizations is applied along a set of directions. Those directions have to be "non-interfering" such that the minimization along one direction is not diminished by the subsequent minimization along another direction. A mutually conjugate set of directions has the desired property. Given a function f , the two vectors u and v are conjugate if

$$u \cdot A \cdot v = 0 \tag{155}$$

where A is the Hessian matrix of f at a point P which serves as the origin of the coordinate system,

$$[A]_{ij} \equiv \frac{\partial^2 f}{\partial x_i \partial x_j} |_P . \tag{156}$$

In other words, the minimization along a new direction v will make the gradient of the function f , which is $\nabla f = A \cdot v$ in this case, stay perpendicular to u . If any two vectors in a given set of directions are conjugate, this set is called mutually conjugate with respect to f . Powell first came up with a procedure for producing N mutually conjugate directions. This procedure is described by the Numerical Recipes [3] as follows:

"Initialize the set of directions u_i to the basis vectors, $u_i = e_i$, $i = 1, \dots, N$, repeat the following sequence of steps until your function stops decreasing:

- Save your starting position as P_0 .
- For $i = 1, \dots, N$ move P_{i-1} to the minimum along direction u_i and call this point P_i .
- For $i = 1, \dots, N - 1$, set $u_i \leftarrow u_{i+1}$.
- Set $u_N \leftarrow P_N - P_0$.
- Move P_N to the minimum along direction u_N and call this point P_0 ."